



저작자표시-비영리-변경금지 2.0 대한민국

이용자는 아래의 조건을 따르는 경우에 한하여 자유롭게

- 이 저작물을 복제, 배포, 전송, 전시, 공연 및 방송할 수 있습니다.

다음과 같은 조건을 따라야 합니다:



저작자표시. 귀하는 원저작자를 표시하여야 합니다.



비영리. 귀하는 이 저작물을 영리 목적으로 이용할 수 없습니다.



변경금지. 귀하는 이 저작물을 개작, 변형 또는 가공할 수 없습니다.

- 귀하는, 이 저작물의 재이용이나 배포의 경우, 이 저작물에 적용된 이용허락조건을 명확하게 나타내어야 합니다.
- 저작권자로부터 별도의 허가를 받으면 이러한 조건들은 적용되지 않습니다.

저작권법에 따른 이용자의 권리는 위의 내용에 의하여 영향을 받지 않습니다.

이것은 [이용허락규약\(Legal Code\)](#)을 이해하기 쉽게 요약한 것입니다.

[Disclaimer](#)

**A THESIS
FOR THE DEGREE OF MASTER OF SCIENCE**

Functional insights into two potent constituents in molluscan physiology, identified from Disk abalone (*Haliotis discus discus*) deciphering their putative significance in host defense.

Herath Mudiyanseelage Lalinka Priyashan Bandara Herath

**Department of Marine Life Science
GRADUATE SCHOOL
JEJU NATIONAL UNIVERSITY
REPUBLIC OF KOREA**

2016.02

Functional insights into two potent constituents in molluscan physiology, identified from Disk abalone (*Haliotis discus discus*) deciphering their putative significance in host defense.

Herath Mudiyansele Lalinka Priyashan Bandara Herath
(Supervised by Professor Jehee Lee)

A thesis submitted in partial fulfillment of the requirement for the degree of

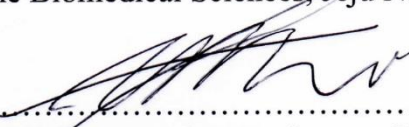
MASTER OF SCIENCE

February 2016

This thesis has been examined and approved by



.....
Thesis director, Qiang Wan (PhD), Research Professor of Marine Life Sciences,
School of Marine Biomedical Sciences, Jeju National University



.....
Chulhong Oh (PhD), Associate Professor of Marine Biology,
Korean Institute of Ocean Science & technology, University of Science & Technology



.....
Jehee Lee (PhD), Professor of Marine Life Sciences,
School of Marine Biomedical Sciences, Jeju National University

Date: 19th of February, 2016

Department of Marine Life Sciences

GRADUATE SCHOOL

JEJU NATIONAL UNIVERSITY

REPUBLIC OF KOREA

Acknowledgements

“Fide it virtue”, from the childhood to now, the motto of my life. I was glad enough to meet such people as my guardians and advisors who apply the same motto to their lives. Without their encouragement, this dissertation might not have been written, and to whom I am greatly indebted.

First and foremost I offer my sincerest gratitude to my supervisor, Professor Jehee Lee for giving me a golden opportunity to conduct my Master studies in the Marine Molecular Genetics Laboratory under his invaluable supervision. Furthermore, I am grateful to him for his enormous support, encouragements, understanding, and patience throughout my study period. Without his timely, insightful contribution, and funding to make my Master studies and life in Korea would not have been possible, and I sincerely would not be here. During my study period, I have adored him as a great advisor, good leader with goal-oriented personality. I am really grateful to have him in my enlighten event of my life.

Secondly, I extent my sincere thanks to Prof. R. S. Dassanayake and DR. N.V. Chandrasekharan for recommending me and DR. Don Anushka Sandaruwan Elvitigala for introducing me to Prof. Jehee Lee.

I would also be thankful to the members of my Master committee, Prof. Chulhong Oh, DR. Qiang Wan who monitored my work and kindly spared their time in reading and providing me with valuable suggestions for making this study an appreciable one.

In addition, I acknowledge with great thanks to the Prof. Gi-Young Kim and DR. Prasad Jayasooriya for the great support given through my Master thesis.

I am also thankful to DR. Bong-Soo Lim and DR. Hyung-Bok Jung and other members of Fish vaccine research center of Jeju National University, who gave kind support during field and laboratory experiments of my study.

It is a great experience and pleasure to spend my study life with past and present colleagues of our laboratory and I am thankful to Ms Eunyoung , Ms Jiyeon , Dr. Hwang, Dr. Jung, Dr. Lim, Dr. Jin, Dr. Umasuthan, Ms. Sukkyoung, Mr. Yucheol, Mrs. Thulasitha, Mr. Thiunuwan, Ms. Minyoung, Mr. Seongdo, Mr. Viraj, Mr. Handun, Ms. Mothishri, Ms. Jeongin, Ms. Sunhye, Ms. Gabin, Mrs. Nadeesahni, Mr. Sachith, Mr. Kugapreethan Ms. Jeongeun and Ms. Hyowon. Again I would like to thank all the Sri Lankan members in Jeju National University (JNU), Mr. Buddhi, Mr. Susara, Mrs. Dilshara, Mrs. Hamsanandini, Mr. Lakmal, Mr. Malintha, Mr. Madusahn, Mr. Shanura, Mr. Asanka and Mrs. Madhushani and David for their encouragements in my research Works and sharing their kindness and friendship with me.

I am indebted to all the members of Jeju National University International Student organization, for their strength and encouragement especially to Prof. Young-Hoon Kang, The Dean, Center of International Affairs, and his team members, for their help and hospitality. A special thank goes to miss. Eunyeong oh for the outright support given to me to act as the President of JNU International Student organization (JISO) while completing my academic studies.

I am also grateful to Department of Marine Life Sciences for providing me a peaceful environment for my academic and research works. Further I thank to our group of administrative people, who always willing to help me in administrative works.

I thank Brain Korea 21 and National Fisheries Research and Development Institute Grant, which provided the funds for presenting the research works.

I take this opportunity to thanks all Korean and international students who support me during my stay at student dormitory and the officials of student dormitory office for their kind hospitality.

I would like to thank all those whom I have not mentioned above but helped me in numerous ways to my success.

My deepest gratitude goes to my loving parents (Mr. Wasantha Herath, Mrs. Damayanthi Herath, Mr. Nissanka, Herath, Mrs. Deepani Herath, Imalka Herath, Manilka Herath, Tharuka Herath, and Yasara Herath) for their unflagging love and support; this dissertation is simply impossible without them.

Last but not least, I would like to express my eternal appreciation to my ever loving fillip, Dinithi Doranagoda, for her invaluable encouragements, supports gave to me at every time during my Master study period. Your patience and understanding is amazing. You cheered me on and on.

CONTENTS

Summary in Korean (요약문)

Summary

List of figures

List of tables

Introduction

01

CHAPTER I: Molecular insights into a molluscan transferrin homolog identified from disk abalone (*Haliotis discus discus*) evidencing its detectable role in host antibacterial defense

| | |
|---|----|
| 1. Abstract | 13 |
| 2. Material and Methodology | |
| 2.1. Identification of <i>AbTrf</i> cDNA from a transcriptome database | 14 |
| 2.2. Sequence characterization and evolutionary analysis | 14 |
| 2.3. Overexpression of the recombinant abalone transferrin N-terminal domain (rAbTrf-N) | 15 |
| 2.4. Iron-binding assay of rAbTrf-N protein (chrome azurol S assay, CAS) | 17 |
| 2.5. Shellfish rearing for the immune challenge experiment | 17 |
| 2.6. Immune challenge experiment, RNA extraction, and cDNA synthesis | 18 |
| 2.7. Quantitative real time PCR (qPCR) analysis of mRNA expression levels | 19 |
| 2.8. Antibacterial assay for rAbTrf-N | 20 |
| 3. Result and Discussion | |
| 3.1. Identification and bioinformatics characterization of <i>AbTrf</i> cDNA sequence and the derived amino acid sequence | 21 |
| 3.2. Sequence homology and phylogenetic analysis of abalone transferrin amino acid sequence | 25 |
| 3.3. Putative functional prediction of AbTrf based on the construction of the 3D structure | 29 |
| 3.4. Functional assessment of the putative AbTrf-N protein in Fe ³⁺ binding using purified recombinant AbTrf-N protein | 31 |
| 3.5 Tissue specific expression of <i>AbTrf</i> mRNA | 34 |
| 3.6. Modulation of <i>AbTrf</i> mRNA profile upon pathogenic challenge conditions | 35 |
| 3.7. Investigation of antimicrobial property of AbTrf-N | 38 |

CHAPTER II: Molecular identification and functional delineation of a glutathione reductase similitude from Disk abalone (*Haliotis discus discus*): insights as a potent player in host antioxidant defense

| | |
|---|-----------|
| 1. Abstract | 43 |
| 2. Material and Methodology | |
| 2.1. Identification of <i>AbGSR</i> cDNA from cDNA database | 44 |
| 2.2. Sequence characterization, evolutionary relationships and structural prediction of <i>AbGSR</i> | 45 |
| 2.3 Recombinant expression and purification of putative <i>AbGSR</i> protein | 46 |
| 2.4. GSR specific enzymatic assay, assessment of enzymatic properties of r<i>AbGSR</i> and inhibitory effect of metal ions | |
| 2.4.1. Glutathione reductase activity assay | 48 |
| 2.4.2. Enzymatic properties determination | 48 |
| 2.4.3. Effect of heavy metals on r<i>AbGSR</i> activity | 49 |
| 2.5. Antioxidant properties of r<i>AbGSR</i> | |
| 2.5.1. Disk diffusion assay | 49 |
| 2.5.2. Cell culture and cell viability assays | |
| 2.5.2.1. MTT assay | 50 |
| 2.5.2.2. Flow cytometry | 51 |
| 2.6. Investigation of immune related mRNA expression pattern of <i>AbGSR</i> | |
| 2.6.1. Animal rearing | 51 |
| 2.6.2. Immune challenge experiment, RNA extraction and cDNA synthesis | 52 |
| 2.6.3. Quantitative real time PCR (qPCR) analysis of mRNA expression levels | 53 |
| 2.7. Statistical analysis | 54 |
| 3. Results and Discussion | |
| 3.1. Sequence identification and Bioinformatics analysis of <i>AbGSR</i> cDNA and predicted amino acid sequences | 54 |
| 3.2. Sequence homology and evolutionary analysis | 55 |
| 3.3. The functional interpretation of <i>AbGSR</i> based on 3D structural features | 60 |
| 3.4. Overexpression and functional properties confirmation of recombinant <i>AbGSR</i> protein | 61 |
| 3.5. Enzymatic properties validation and effect of heavy metals on r<i>AbGSR</i> activity | 64 |
| 3.6. Involvement of <i>AbGSR</i> in antioxidant defense mechanisms | 67 |
| 3.7. qPCR analysis of <i>AbGSR</i> tissue specific mRNA expression and immune related expression patterns | 72 |
| 3.8. Conclusion. | 75 |
| References | 83 |

Summary in Korean (요약문)

해양 생물은 그들의 생리학적 메커니즘에 영향을 주는 다양한 환경요인에 노출되어있으며 이러한 요인에 저항하기 위해서 다양한 방어기전을 수행해야 한다. 전복은 주요 양식 진미품으로서 상업적으로 매우 가치가 크다. 또한, 해양 무척추 연체동물 패류에 속하는 종으로 병원균 감염에 대해 독특한 면역 메커니즘과 생체 내 불균형을 일으키는 다양한 요인에 저항하는 생화학적 메커니즘을 가진다.

최근 전복의 유전현상에 관한 연구는 많이 진행되고 있지만, 다양한 스트레스 환경에서의 숙주 방어 능력에 관한 연구는 많지 않다. 따라서 이 연구에서는 전복의 방어체계에서 중요한 분자 구성성분인 박테리아로부터 숙주를 보호하는 transferrin, 항독성 기능을하는 glutathione reductase 유전자를 분자학적 및 기능학적으로 동정하였다.

Transferrin의 기본적인 기능은 3가 철이온과 결합하는것으로 대사과정이 일어나는 장소로 그들을 운반하는 역할을 하며, 면역반응에도 관여한다. 이러한 이유로 transferrin은 숙주 면역에있어 중요한 급성 단백질로 알려졌다. 이 연구에서 동근전복 transferrin like 유전자 (*AbTrf*)를 분자학적 및 기능학적으로 동정하였다. *AbTrf*는 728개의 아미노산을 암호화하는 2189 bp의 ORF로 구성되었으며, 아미노산의 N-말단 부분과 C-말단 부분의 transferrin like domain, 철이온과의 결합을 위한 active site, 보존된 시스테인 잔기가 존재하였다. qPCR을 수행하여 *AbTrf*의 조직별 발현을 분석한 결과, 맨틀과 근육에서 높은 발현을 보였다. *Vibrio parahaemolyticus*, *Listeria monocytogenes*, LPS로 인위감염시킨 전복의 아가미와 혈구에서 *AbTrf* mRNA의 발현이 증가하였다. Transferrin N-말단 도메인의 재조합 단백질은 chrome azurol S (CAS) assay 통해 단백질 농도에 따라 철 3가 이온의 결합능이 비례함을 보였다. 그리고 철에 의존적인 *Escherichia coli*의 성장은 억제하였지만 *Lactobacillus plantarum*의 성장을 억제하지는 못했다. 실험결과들을 종합해보면, *AbTrf*는 병원균으로부터 철이온을 뺏음으로써 숙주의 선천면역에 중요한 역할을 하는것으로 생각된다.

Glutathione reductase은 산화형 glutathione을 환원형으로의 반응을 촉매하는 효소이다. 환원형이 과산화수소에대한 항독성에 중요한 기능을 하기 때문에 산화형과 환원형의 비율은 중요하며, 이를 위해 glutathione reductase은 필수적이다. 이 연구에서는 동근전복 glutathione reductase (*AbGSR*)의 분자학적 및 기능학적으로 동정하였다. 909개의 아미노산을 암호화하는 2325 bp의 ORF로 구성되었으며, 아미노산에 pyridine nucleotide-disulphide oxidoreductase domain, pyridine nucleotide-disulphide oxidoreductase dimerization domain, rossmann-fold NAD(P)(+)-binding proteins superfamily signature가 존재하였다. 4개의 기능적인 잔기인 FAD binding site, glutathione binding site, NADPH binding motif와 assembly domain도 잘 보존된것을 확인하였다. glutathione 재조합 단백질로 glutathione reductase 활성 실험을 수행하였다. 최적의 pH와 온도는 7.0 pH와 50°C로 측정되었으며, 각각 배지의 이온강도에 대해 어떤 효과도 나타내지 않았고, 효소활성은 Cu^{+2} 과 Cd^{+2} 이온에 의해 억제되었다. Disk diffusion assay 결과 세포 보호 효과를 보여주었고, MTT assay와 flow cytometry를 통해서도 상당한 세포 보호 효과를 나타냈다. *AbGSR*은 전복의 다양한 조직에서 발현되었으며,

Vibrio parahaemolyticus, *Listeria monocytogenes* , LPS 로 인위감염시킨 경우 AbGSR 의 발현이 유도되었다. 종합적으로, AbGSR 은 숙주 방어체제를 중재하는 항독성에서 매우 중요한 역할을 하는것으로 보인다.

Summary

The marine species including fish and shellfish are frequently encountered with different environmental factors which affect the proper functionality of normal physiological mechanisms. To defy these environmental conditions, marine organisms need to carry different kind of host defense mechanisms and strong resistance to extreme environmental conditions. When it comes to shellfish aqua farming, abalone is identified as one of the main delicacy which can exclusively be obtained by aquaculture methods. Abalone as a “marine invertebrate molluscan shellfish species”, needs to be equipped with unique types of host defense mechanisms against pathogenic infections and a range of biochemical mechanisms to be resisted against different environmental factors that possibly can imbalance the normal physiology of animal.

Even though currently undergoing researches on abalone physiology focus only on the general phenomena, not much studies are undergoing on the uncommon mechanisms which can provide outstanding host defensive abilities and survival capabilities under septic and different stress conditions, and yet to be properly investigated in order to reveal the valuable piece of hidden knowledge. In the presence of so called background, we design the current study to molecularly identify and functionally annotate the uncommon physiological molecular components which are not yet identified from abalone. As a preliminary approach to start this worthwhile contrive, in this thesis I have extensively characterized a transferrin homolog identified from our disk abalone (*Haliotis discus discus*) database which capacities an indirect but significant involvement in an antibacterial host defense mechanisms. Moreover, I direct the current study to identify a homolog of glutathione reductase from our database which is not extensively studied in molluscan family,

in order to investigate the essence of having antioxidants defense systems in shellfish species such as abalones.

The basic function of transferrin is to bind iron (III) ions in the medium and to deliver them to the locations where they are required for metabolic processes. It also takes part in the host immune defense mainly via its ability to bind to iron (III) ions. Hence, transferrin is also identified as an important acute-phase protein in host immunity. Since transferrin is known to be a major player in innate immunity, in the present study we sought to identify, and molecularly and functionally characterize a transferrin-like gene from disk abalone (*Haliotis discus discus*) named as *AbTrf*. *AbTrf* consisted of a 2187-bp open reading frame (ORF) which encodes a 728 amino acid (aa) protein. The putative amino acid sequence of *AbTrf* harbored N- and C-terminal transferrin-like domains, active sites for iron binding, and conserved cysteine residues. A constitutive tissue specific *AbTrf* expression pattern was detected by qPCR in abalones where mantle and muscle showed high *AbTrf* expression levels. Three immune challenge experiments were conducted using *Vibrio parahaemolyticus*, *Listeria monocytogenes* and LPS as stimuli and, subsequently, *AbTrf* mRNA expression levels were quantified in gill and hemocytes in a time-course manner. The mRNA expression was greatly induced in both tissues in response to both challenges. Evidencing the functional property of transferrins, recombinant *AbTrf* N-terminal domain (*AbTrf*-N) showed dose-dependent iron (III) binding activity detected by chrome azurol S (CAS) assay system. Moreover, recombinant *AbTrf*-N could significantly inhibit the growth of iron-dependent bacterium, *Escherichia coli* in a dose-dependent manner. However, *AbTrf*-N was unable to show any detectable bacteriostatic activity against iron-independent bacterium *Lactobacillus plantarum* (*L. plantarum*) even at its highest concentration. Collectively, our results suggest that *AbTrf* might play a significant role in the host innate immunity, possibly by withholding iron from pathogens.

Glutathione reductase (GSR) as an enzyme catalyzes the biochemical conversion of glutathione oxidized form (GSSG) into reduced form (GSH). Since ratio between two forms of glutathione (GSH/GSSG) is important for the proper functioning of GSH to act as an antioxidant against H₂O₂, contribution of GSR is essential. We conducted the current study to reveal the molecular and functional properties of GSR similitude identified from disk abalones (*Haliotis discus discus*). The identified cDNA sequence (2325 bp) bears a 1356 bp long ORF, coding for a 909 bp long amino acid sequence which harbored a pyridine nucleotide – disulphide oxidoreductase domain (171-246 aa), a Pyridine nucleotide-disulphide oxidoreductase dimerization domain and a Rossmann-fold NAD(P)(+)- binding proteins superfamily signature. Four functional residues; FAD binding site, glutathione binding site, NADPH binding motif and assembly domain were identified to be conserved among the other species. The recombinant AbGSR (rAbGSR) exhibited a detectable activity with standard glutathione reductase activity assay. The optimum pH and optimum temperature for the reaction were detected at 7.0 pH and 50 °C, respectively while showing no effect of the ionic strength of the medium. The enzymatic reaction was vastly inhibited by Cu⁺² and Cd⁺² ions. A considerable cell protective effect was detected with disk diffusion assay conducted with rAbGSR. Moreover, with MTT assay and flow cytometry, significance of cell protectiveness provided by rAbGSR was confirmed. Moreover, *AbGSR* was found to be ubiquitously distributed in different types of abalone tissues. *AbGSR* mRNA expression exhibited the potent inductions in three immune challenges conducted with *Vibrio parahaemolyticus*, *Listeria monocytogenes* and LPS predicting its possible involvements in host defense mechanisms under pathogenic infections. Taken together, results of current study suggest that AbGSR might play an important role in antioxidant mediated host defense mechanisms while providing insights into immunological contribution of AbGSR.

List of figures

Fig. 1: ClustalW multiple sequence alignment of the deduced amino acid sequences of AbTrf with known Trf proteins.

Fig. 2: Phylogenetic analysis of AbTrf with selected known full-length Trf amino acid sequences of other species.

Fig. 3: Tertiary structure of AbTrf according to the homology based modeling strategy.

Fig. 4: SDS-PAGE analysis of rAbTrf-N protein.

Fig. 5: Iron-binding activity of rAbTrf-N using standard CAS assay.

Fig. 6: Tissue specific mRNA expressions of *AbTrf* determined by qPCR.

Fig. 7: Transcriptional expression profiles of *AbTrf* mRNA (**A**) in gill tissue and (**B**) in hemocytes.

Fig. 8: The bacteriostatic activity of rAbTrf. (**A**) The growth curve of *E. coli*. (**B**) The growth curve of *Lactobacillus plantarum*.

Fig. 9: ClustalW multiple sequence alignment of the deduced amino acid sequences of AbGSR with known GSR proteins.

Fig. 10: Phylogenetic analysis of AbGSR with selected known full-length GSR amino acid sequences of other species.

Fig. 11: Tertiary structure of AbGSR according to the homology based modeling strategy.

Fig. 12: SDS-PAGE analysis of rAbGSR protein.

Fig. 13: Standard glutathione reductase activity assay using Biovision glutathione reductase activity colorimetric assay kit.

Fig. 14: The enzymatic properties of rAbGSR protein.

Fig. 15: The antioxidant properties of AbGSR protein.

Fig. 16: rMBP and rAbGSR overexpressed in ER2523 cells and plated on LB/Amp agar plates.

Fig. 17: The microscopic observation of the cell sample treated for flow cytometry analysis.

Fig. 18: Tissue specific mRNA expressions of *AbGSR* determined by qPCR.

Fig. 19: Transcriptional expression profiles of *AbGSR* mRNA in hemocytes upon immune stimulation with *Vibrio parahaemolyticus*, *Listeria monocytogenes* and LPS.

List of tables

Table. 1: Oligomers used in this study (for AbTrf)

Table.2: Amino acid identity and similarity of AbTrf entire sequence to other homologs

Table 3: Oligomers used in this study (AbGSR)

Table 4: pairwise sequence alignment (for AbGSR)

INTRODUCTION

Abalone; as a member of phylum Mollusca

Generally phylum Mollusca is the family which includes organisms such as snails, octopuses, squid, clams, scallops, oysters, and chitons. The common feature of molluscans is to have soft bodies which typically have a "head" and a "foot" region. Moreover, distinguishable appendages such as a mantle and an anterior head are well defined. Classification of the members of phylum Mollusca is much complex compared to the others since this phylum includes a diverse range of organisms. Up to date, phylum Mollusca is subdivided into 7 classes of organisms.

Classification of phylum Mollusca

| Class | Species types |
|-----------------------|--|
| Bivalvia | Scallops, clams, mussels, etc. |
| Monoplacophora | Limpet-like “living fossils” |
| Gastropoda | Snails, slugs, limpets Sea hares |
| Cephalopoda | Squids, octopuses, nautilus, ammonites |
| Scaphopoda | Tusk shells |
| Aplacophoda | Spicule- covered, worm- like animals |
| Polyplacophoda | Chitons |

The experimental animal (abalone) that we have studied in current study is predominantly identified as a marine organism which lays in to the gastropod class of phylum Mollusca. Specifically as a gastropod, abalone contains one shell as a deviating characteristic from bivalves. Shell contains a row of respiratory pores on its shell surface. Abalones are capable of attaching to the rocky surfaces due to the suction power of their muscular foot. The muscle attached to the shell is known as shell muscle. Mantle circles the foot as an extended part of foot and bears tentacles.

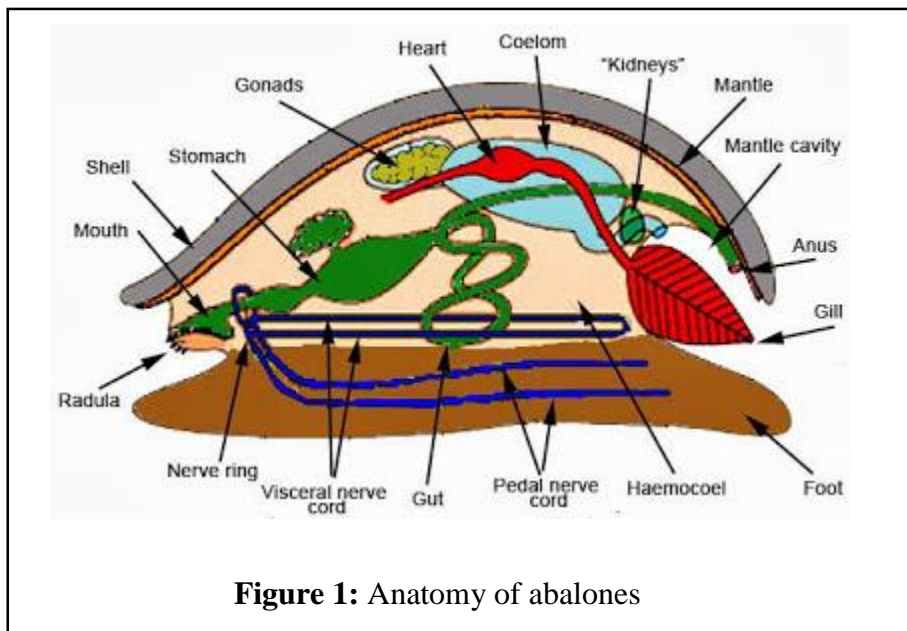


Figure 1: Anatomy of abalones

Up to date, there are several types of abalone species have been identified from different areas of world.

Haliotis asinina, *Haliotis discus*, *Haliotis discus hannai*, *Haliotis diversicolor supertexta*, *Haliotis fulgens*, *Haliotis iris*, *Haliotis kamtschatkana*, *Haliotis laevigata*, *Haliotis midae*, *Haliotis rubra*, *Haliotis rufescens*, *Haliotis tuberculata*, *Haliotis laevigata*, and *Haliotis rubra*

Insights into abalone host defense and stress tolerating mechanisms

The animal species inhabited in marine biota are vastly exposed to a different kind of environmental stresses such as pathogenic challenges, oxidative stresses, pH changes, temperature changes, mechanical stresses, salinity differences etc. To withstand such challenges, marine organisms need to bear advanced defensive mechanisms and an outstanding resistance against stresses.

The immune system is the affiliated body to protect an animal from pathogenic infections. It can mainly be divided into two arms; adaptive immunity system and innate immunity system. The adaptive immunity is also known as the acquired immune system and consisted of highly specific systemic cells and mechanisms that can eliminate or prevent pathogens growth. The adaptive immune responses may last for a long period of time with an immune memory for infectious diseases. The innate arm of immunity is consisted of non-specific host defense mechanisms and molecular components that protect the host organism by preventing pathogenic invasions and establishment of infections in host tissues. It provides protection to the host in a universal manner while protecting against vast range of infections, without being specific and bearing a memory against particular type of infections. In vertebrates both adaptive and innate immunological components are seen, while in invertebrates only the components in the innate immunity are presence.

Reactive oxygen species (ROS) production tend to exceed the cutoff levels due to various environmental factors. Antioxidant defense mechanisms exhibit its involvement to protect host from harmful free radical generation. In antioxidant defense mechanisms, various type of proteins

and non-protein antioxidant species act together to prevent oxidation of cellular component and in turn apoptosis taken place at cellular level. To be survived under different environmental conditions such as high temperatures, some marine organisms contain different types of hyperthermophilic enzymes (thermostable) to ensure the proper functionality of important biochemical mechanisms. Halophiles, which have high tolerance levels to extreme salinity conditions can survive in different areas of marine environments.

Collectively, all the aforementioned mechanisms provide a considerable contribution to a marine organism to survive overcoming different environmental challenges. Since abalone is an invertebrate marine shellfish species, their innate immunological mechanisms seem to be prominent in order to protect them from pathogenic infections. Since abalones are frequently encountering with different environmental factors that trigger the production of ROS including pathogenic infections, presence of strong antioxidant mechanisms are a prerequisite.

Entrance and Foundation for the current study

Shellfish species inhabited in marine biota are widely exposed to a vast range of disease causing bacterial (Huang et al., 2001; Liu et al., 2000), viral (Nakatsugawa et al., 1999) and parasitic (Goggin and Lester, 1995) species. Owing to this cause, mari-cultured shellfish are hypersensitive to infectious diseases (Elston and Lock wood, 1983), which possibly can only be controlled by innovative methods. At the same time, shellfish, as marine organisms are exposed to a vast range of toxic substances such as heavy metals, which in turn may cause imbalance in the general physiology of shellfish by interacting with important biochemical reactions. Collectively,

interactions with microorganisms and other foreign materials cause a huge production loss in aquaculture.

In order to establish sophisticated and expanded technologies in shellfish aquaculture, it is important to incorporate novel insights into the molecular and biochemical mechanisms which have responsible roles in host defense via, yet unrevealed pathways under environmental stress and pathogenic conditions. Abalone, a shellfish species, has been trended as a highly demanded aqua crop particularly as a delicacy (Cook, 2014). Since abalone is susceptible for a wide range of environmental factors, which possibly can cause imbalance in the general physiology of abalone, it is now a markedly trending factor to analyze the general biochemical pathways and immunological mechanisms in abalone at a molecular biological platform (Evans et al., 2000; Klinbunga et al., 2003; Wan et al., 2012).

As a primary step to answer the major problems associated with abalone production losses, it is very important to analyze and annotate molecular components that has a significant involvement in abalone host defense. Knowledge untangled from these studies may further manipulated to build up new technologies in abalone aquaculture. Therefore, in current study we have gathered molecular insights on two important molecules; one is identified as an important innate immunological counterpart (Transferrin protein) and other is a potent player in antioxidant defense mechanism (Glutathione reductase enzyme).

Transferrin gene.

The protein transferrin is an indispensable molecular component of the innate immune system of most vertebrates and invertebrates (Lambert et al., 2005a). In the host, the level of freely available iron (III) ions in most biological fluids are extremely low since iron (III) is bound by transferrin with high affinity (Uribe et al., 2011). Thus, transferrin shows antimicrobial activity against a vast range of Gram-positive and Gram-negative bacteria by sequestering the available free ferric iron in cellular media which is essential for microbial survival or growth (Liu et al., 2009). Once the pathogen invades the host, in order to establish an infection, the pathogen must possess the ability to successfully propagate in the host's body fluids (Casadevall and Pirofski, 2001). Meanwhile, to establish a higher level of virulence, pathogens should produce a range of virulence determinants, which are affected by different environmental factors (Casadevall and Pirofski, 2001). Out of these environmental factors, the presence of an optimum iron level is one of the crucial factors for the synthesis of some of the virulence determinants (Patel and Carr, 2008). Hence, transferrin functions as a regulatory molecule in the expression of toxins and other bacterial virulence determinants, despite its primary role in the regulation of the iron acquisition machinery (Aisen, 1989).

Transferrin is a family of proteins, which comprises single chain non-heme iron-binding β -globulin proteins (Brown et al., 1982). Depending on its location in the body, and its structural and functional properties, transferrin is categorized under several sub-classes including serum transferrin (Stf), ovotransferrin (Otf), lactoferrin (Ltf), melanotransferrin (Mtf), and other Trf-like proteins (Brown et al., 1982). Transferrin was first identified as a serum protein in humans, capable of binding serum iron (III) (Fe^{3+}) ions, in order to remove them from the medium (Aisen, 2004).

The greater fraction of freely available iron (III) present in the serum binds to apo-transferrin and changes the conformation of transferrin to the closed form (formation of the Fe^{3+} -Trf complex) making possible its internalization via receptor-mediated endocytosis of the transferrin receptor. Subsequently, iron (III) molecules participate in a wide variety of cellular metabolic processes serving as electron donors or acceptors (Gomme et al., 2005). This process indirectly helps to regulate the iron level in biological fluids. In biochemical terms, transferrin is a glycoprotein (Aisen, 2004; Gomme et al., 2005) and contains two main structural domains: an N-terminal domain and a C-terminal domain. These two domains are interconnected by a short stretch of amino acids and each lobe has two further sub-regions (N1 and N2 in the N-terminal domain, and C1 and C2 in C-terminal domain) (Wally et al., 2006). In addition, transferrin has central iron-binding (Fe^{3+}) cavities located in both N-terminal and C-terminal domains (Noinaj et al., 2012). The formation of two identical domains is believed to be due to gene duplication events that occurred during molecular evolutionary processes (Jamroz et al., 1993; Nichol et al., 2002). Comprehensive studies on transferrin indicate that most of the C-terminal domains from insect transferrins lack the ability to bind to iron since functionally important amino acid residues have been substituted by different amino acids; however, the transferrins from some insects including *Blaberus discoidalis* (Jamroz et al., 1993), the termite *Mastotermes darwiniensis* (Thompson et al., 2003), the beetle *Apriona germari* (Lee et al., 2006), and *Protatetia brevitarsis* (Kim et al., 2008) carry bilobed iron-binding features similar to those present in mammalian transferrins. In addition, some transferrin-like molecules have been documented to contain one lobe (single-lobed transferrins) or three lobes (trilobed transferrins) with iron (III) binding ability (Lambert et al., 2005b).

Diverse structural features have been observed among the transferrin-like proteins identified to date. A recent bilobed transferrin-like homolog has been identified in amphioxus but with additional intervening sequence in the C-terminal lobe (Liu et al., 2009). A pacifastin protein from *Macrobrachium rosenbergii* contains a unique four-lobed structure (Toe et al., 2012). Transferrin-like major yolk proteins have been identified in sea urchins (Brooks and Wessel, 2002). Saxiphilins of frogs show several characteristics of transferrin (Lenarcic et al., 2000; Morabito and Moczydlowski, 1994). Otolith matrix protein 1 in fish was also detected to have transferrin-like characteristics in their tertiary structures (Murayama et al., 2000).

The biological importance of transferrin encompasses physiological and immunological properties due to its iron-binding ability. From the studies to date, transferrin has been identified as a well distinguishable part of the innate immunity. Mainly, it shows an antimicrobial property by binding to iron, hence, sequestering the iron needed for the survival and proliferation of invading pathogens (Ong et al., 2006). According to the studies on goldfish and carp, transferrin is a primary activating agent of macrophage-mediated antimicrobial responses (Jurecka et al., 2009; Stafford and Belosevic, 2003; Stafford et al., 2001). Thus, transferrin-derived synthetic peptides could induce pro-inflammatory responses in macrophages.

Glutathione reductase gene

In biological systems, formation and overproduction of reactive oxygen species (ROS) is being triggered by a variable range of environmental factors (Valko et al., 2006). In contrast, the reactions mediated by antioxidants seemed to be involved in counterbalancing the harmful effect of ROS (Seifried et al., 2007). Antioxidants primarily function as molecular components to inhibit

the oxidation of other molecules from ROS (Birben et al., 2012). So that, antioxidants are generally grouped in the chemical groups of thiols, ascorbic acid, or polyphenols which are capable to be self-oxidized by interacting with ROS (Sies, 1997).

In the sense of the important cellular processes such as mitogenic stimulation or cell cycle regulation, H_2O_2 is identified as a most important ROS type (Munoz et al., 2002). But excessive production of H_2O_2 may cause oxidative damage to the inner cellular components. Therefore, intracellular H_2O_2 should be present at biologically controlled levels. The harmful free radical generation is happening not only in the cytoplasm of cells but also in the small organelle such as mitochondria (Cadenas and Davies, 2000; Sanz and Stefanatos, 2008). Since mitochondria is recognized as the power generator for the biological processes undergoing at cellular level, it generates the conserved form of energy via the process of oxidative phosphorylation, linking with the energy-releasing activities of electron transport and proton pumping (Alberts et al., 2002). The potential side reactions that occur coupling with electron transport chain are known to generate superoxide anion radicals ($O_2^{\cdot-}$) which eventually get converted into H_2O_2 molecules. These H_2O_2 can cause the oxidative damages to mitochondrial membranes and inner materials that can impair the central energy generative mechanisms of cells (Boveris, 1977).

Glutathione is a biologically dispersed pivotal antioxidant counterpart which is categorized under thiol family, and directly interacts with H_2O_2 to reduce them into biochemically stable forms of H_2O and O_2 (Meister, 1988; Presnell et al., 2013). More confining insights into the biochemical mechanism show that reduced form of glutathione (GSH) reacts with H_2O_2 via an enzymatic process catalyzed by glutathione peroxidase (Toppo et al., 2009). Once the reaction is on progress, available GSH is converted into oxidized form of glutathione (GSSG). Hence, continuous

regeneration of GSH from GSSG is a compulsory phenomenon to ensure that the eliminating process of H_2O_2 is maintained in continuous manner.

The regeneration of GSH from GSSG is controlled by a supplementary enzymatic reaction which is catalyzed by an enzyme glutathione reductase also known as glutathione disulfide reductase (GSR). As of GSR is the regulating factor to the reaction, it helps to maintain the body GSH/GSSG ratio in an optimal level, which is a parameter of oxidative stress as well as change

s in redox signaling and control (Jones, 2002). In stepwise manner, mechanism of corresponding catalytic reaction is going through two distinguishable phases; first portion is a reductive half and second portion is an oxidative half (Jones, 2002).

Human GSR executes its function as a homodimer in which each monomeric size is 52 kDa (Karplus and Schulz, 1987). Functionally, GSR has an indirect contribution towards the diverse biological processes via glutathione, despite its primary function is to act as a crucial member in glutathione metabolism. Human glutathione is widely studied and identified to be present in detoxification mechanisms of xenobiotics (Sipes et al., 1986), as a cofactor in isomerization reactions (Pettersson and Mannervik, 2001) and as a storing and transporting agent of essential cysteine amino acid residues (Volodymyr 2012) etc. Moreover, recent studies reveal that the GSH levels have an interference with the cell proliferation mechanisms and regulatory mechanisms of apoptosis (Day and Suzuki, 2005).

In septic conditions, H_2O_2 exceeds the basal levels as a response to pathogenic infection. To revert the exceeding H_2O_2 levels to the basal, expression of GSR gene is a prerequisite since GSR enzyme bears a predominant role in the process of eliminating H_2O_2 from the medium. And also with

mammalian studies, it is now a well identified fact that glutathione reductase is an essential player in defense of host against the bacterial infections (Yan et al., 2013).

To the date, a glutathione reductase homolog has been identified and extensively analyzed, from lower vertebrate fish species rainbow trout (Tekman et al., 2008). With respect to invertebrates, direct molecular characterizations and expression analysis of GSR has been conducted with species such as *Onchocerca volvulus* (Muller et al., 1997). Moreover, studies have been conducted to molecularly identify and detect the expression of GSR upon different types of environmental stressors (Seo et al., 2006). In spite of aforementioned indicates with respect to animals, glutathione reductase has also been identified to bear a pivotal role in plant physiology (Gill et al., 2013). However, even though GSR shares an important role in antioxidant defense mechanisms equally in animal and plant biota, none of the molluscan counterparts have been characterized at molecular and functional level to investigate antioxidant properties. So that, the current study has taken effort towards the characterization of an invertebrate GSR homolog from molluscs, at molecular and functional level.

Identification of abalone transferrin and glutathione reductase, and specific approaches for characterization

In the current study, we identified putative orthologs of transferrin from our disk abalone (*Haliotis discus discus*) cDNA database. This is the first time that such effort has been carried out in gastropods. Its involvement in immunity was analyzed based on its mRNA expressional level upon different types of pathological conditions. Further, in order to clarify the

functional involvement of the identified transferrin ortholog in antimicrobial activities, biochemical studies were conducted to analyze its possible involvement in iron III (Fe^{3+}) binding and, thus, its putative antimicrobial properties through its iron-binding ability. Specifically, as a novel approach, we sought to validate the antibacterial characteristic of the abalone transferrin N terminal domain (AbTrf -N) using two bacterial species: *Escherichia coli* (*E. coli*) and *Lactobacillus plantarum* (*L. plantarum*) which are iron dependent and iron independent, respectively, for activities such as growth, proliferation, and mediation of virulence. In addition, the antimicrobial activity against these two types of bacterial strains was compared while demonstrating the need for iron for microbial growth.

Moreover, we identified a glutathione reductase (AbGSR) similitude from above mentioned similar disk abalone (*Haliotis discus discus*) transcriptomic database. The AbGSR counterpart was annotated at cDNA and amino acid levels using molecular bioinformatics tools. The recombinant protein was expressed by adapting recombinant molecular biological technologies, and functional assays were conducted in order to characterize AbGSR counterpart at functional level; to examine the enzymatic properties, and to determine the inhibitory effect of heavy metal ions on AbGSR functionality. Particularly, to interrelate the AbGSR general function with antioxidant properties, experiments were conducted by measuring the cell protective effect of putative AbGSR under the oxidative stress conditions mounted by H_2O_2 . Ultimately, transcriptional levels of AbGSR were quantified at normal physiological conditions, and pathological conditions to investigate the putative involvement of AbGSR in abalone innate immunity.

CHAPTER I:

Molecular insights into a molluscan transferrin homolog identified from disk abalone (*Haliotis discus discus*) evidencing its detectable role in host antibacterial defense

3. Abstract

The basic function of transferrin is to bind iron (III) ions in the medium and to deliver them to the locations where they are required for metabolic processes. It also takes part in the host immune defense mainly via its ability to bind to iron (III) ions. Hence, transferrin is also identified as an important acute-phase protein in host immunity. Abalones are major shellfish aquaculture crops that are susceptible to a range of marine microbial infections. Since transferrin is known to be a major player in innate immunity, in the present study we sought to identify, and molecularly and functionally characterize a transferrin-like gene from disk abalone (*Haliotis discus discus*) named as *AbTrf*. *AbTrf* consisted of a 2187-bp open reading frame (ORF) which encodes a 728 amino acid (aa) protein. The putative amino acid sequence of AbTrf harbored N- and C-terminal transferrin-like domains, active sites for iron binding, and conserved cysteine residues. A constitutive tissue specific *AbTrf* expression pattern was detected by qPCR in abalones where mantle and muscle showed high *AbTrf* expression levels. Three immune challenge experiments were conducted using *Vibrio parahaemolyticus*, *Listeria monocytogenes* and LPS as stimuli and, subsequently, *AbTrf* mRNA expression levels were quantified in gill and hemocytes in a time-course manner. The mRNA expression was greatly induced in both tissues in response to both challenges. Evidencing the functional property of transferrins, recombinant AbTrf N-terminal domain (AbTrf-N) showed dose-dependent iron (III) binding activity detected by chrome azurol S (CAS) assay system. Moreover, recombinant AbTrf-N could significantly inhibit the growth of

iron-dependent bacterium, *Escherichia coli* in a dose-dependent manner. However, AbTrf-N was unable to show any detectable bacteriostatic activity against iron-independent bacterium *Lactobacillus plantarum* (*L. plantarum*) even at its highest concentration. Collectively, our results suggest that AbTrf might play a significant role in the host innate immunity, possibly by withholding iron from pathogens.

Key words: Transferrin, abalone, transcriptional analysis, iron binding, antibacterial activity

4. Material and Methodology

2.1. Identification of *AbTrf* cDNA from a transcriptome database

The full-length cDNA sequence of *AbTrf* was identified from the previously described abalone cDNA sequence database (Lee et al., 2011) using the Basic Local Alignment Search Tool (BLAST) (<http://blast.ncbi.nlm.nih.gov/Blast.cgi>). The identified transferrin-like sequence was named *AbTrf*.

2.2. Sequence characterization and evolutionary analysis

DNASist 2.2 program (version 3.0) was used to identify the open reading frame (ORF) from the putative *AbTrf* cDNA sequence and for the subsequent analysis of the corresponding amino acid sequence. NCBI-BLAST search tool (<http://blast.ncbi.nlm.nih.gov/Blast.cgi>) was used to list the homologous protein sequences for *AbTrf*. Subsequently, pairwise sequence alignment and multiple sequence alignment were performed using EMBOSS needle (https://www.ebi.ac.uk/Tools/psa/emboss_needle/) and ClustalW2 programs, respectively (Thompson et al., 1994). The phylogenetic relationship was determined by the Molecular

Evolutionary Genetics Analysis (MEGA) software version 6 (Tamura et al., 2013) using the neighbor-joining method supported by bootstrapping values taken from 5000 replicates. Characteristic signature domains on AbTrf sequence was predicted by the ExPASy-prosite server (<http://prosite.expasy.org>) and the NCBI conserved domain database (CDD) (Marchler-Bauer et al., 2011). The tertiary structure of the primary AbTrf protein was generated using the online SWISS model interface (Arnold et al., 2006). In this regard, a 2.60 Å resolution crystal structure of full-length, glycosylated apo-human serotransferrin (hTrF) (PDB no.3V83.1.A.pdb) was selected from the PDB database and used as the template for AbTrf. The structural QMEAN4 value for model quality was -8.61. The given 3D structure was represented and analyzed by PyMOL molecular graphic software version 1.3 (WL).

2.3 Overexpression of the recombinant abalone transferrin N-terminal domain (rAbTrf-N)

A sequence-specific forward and reverse primer pair was designed (Table 1) to amplify the cDNA fragment encoding the mature peptide of the AbTrf N-terminal domain. Two adaptor nucleotide sequences which contained *EcoRI* and *HindIII* restriction sites were incorporated to the 5'-ends of the forward and reverse primers, respectively. The PCR reaction was performed in a 50 µL volume of PCR mixture by adding 5 µL of 10× Ex Taq Buffer (with Mg²⁺), 4 µL of 2.5 mM dNTPs, 40 pmol of each primer, 50 ng of liver cDNA, and 5 U of Ex Taq polymerase (TaKaRa). PCR conditions were set as follows: initial denaturation at 94 °C for 3 min, there after 35 cycles of amplification at 94 °C for 30 s, 59 °C for 30 s, and 72 °C for 1.5 min, with a final extension at 72 °C for 5 min. Subsequently, the resulting PCR product was resolved on an agarose gel and purified using an Accuprep™ gel purification kit (Bioneer-Korea).

In order to construct the prokaryotic rAbTrf -N protein expression system, the purified fragment and a prokaryotic expression plasmid, pMALTM-C2X (New England Biolabs, Ipswich, MA, USA), were simultaneously digested with *EcoRI* and *HindIII* and subsequently ligated together using a Mighty Mix DNA Ligation Kit (TaKaRa). To further confirm the accuracy of the recombinant construct (pMAL-C2X/AbTrf-N), the insert in the ligated vector was sequenced (Macrogen-Korea). After sequence confirmation, a recombinant vector was transformed into *Escherichia coli* BL21 competent cells (Novagen).

Transformed BL21 cells were grown in 500 mL of LB broth supplemented with 100 $\mu\text{g mL}^{-1}$ ampicillin and 100 mM glucose at 37 °C until OD₆₀₀ reached ~0.5. Protein induction was then performed by adding isopropyl- β -thiogalactopyranoside (IPTG) to the culture medium at a final concentration of 0.5 mM while maintaining the temperature at 20 °C. Subsequently, the culture was incubated for 12 h at 20 °C. Then, cells were harvested by centrifugation (3500 rpm for 30 min at 4 °C). The supernatant was discarded and the cell pellet was resuspended in a column buffer (20 mM Tris-HCl, pH 7.4, 200 mM NaCl) and kept overnight at -20 °C. The following day, the cell suspension was sonicated on ice in the presence of lysozyme (1 mg/mL). The cell lysate was centrifuged at 9000 $\times g$ for 30 min at 4 °C. Subsequently, the cell pellet was discarded and the supernatant was loaded onto a column packed with amylose resin. After washing the protein bound resin with 10 \times volume of the column buffer, the protein was eluted by adding elution buffer (column buffer + 10 mM maltose). The maltose binding protein (MBP) was also overexpressed by following the above described methodology. The purification process was evaluated by collecting the samples at different steps of purification and loading them into a 12% SDS-PAGE gel along with standard molecular-weight size marker (PageRuler Plus, Thermo

Scientific) and stained with 0.05% Coomassie blue R-250. The protein concentration was measured by the Bradford protein assay (Bradford, 1976).

2.4. Iron-binding assay of rAbTrf-N protein (chrome azurol S assay, CAS)

The method developed by Schwyn and Neilands (1987) was used to assess the iron-binding activity of the rAbTrf-N protein. CAS (chrome azurol S) assay reagent was purchased from Sigma Aldrich (USA). CAS assay solution was prepared according to the method described by Schwyn and Neilands (1987). A concentration gradient of 75, 150, and 300 $\mu\text{g/mL}$ of the recombinant protein or MBP (control) or an equal amount of elution buffer (negative control) was prepared by diluting the purified rAbTrf-N using elution buffer solution. A 500 μL aliquot of the CAS assay solution was mixed with the same amount of rAbTrf-N protein solution. The mixture was incubated at room temperature in the dark for 1 h in order for the reaction to reach equilibrium. After that, the absorbance (OD) was measured at 630 nm. The procedure mentioned above was followed with all protein samples of different concentrations. Ultimately, the relative absorbance (absorbance ratio between the negative control and the samples incubated with proteins) was calculated in order to represent the iron-binding activity of rAbTrf-N as the mean of triplicated assays.

2.5. Shellfish rearing for the immune challenge experiment

Healthy disk abalones were purchased from the Youngsoo commercial abalone farm in Jeju Island, Republic of Korea, and abalones with an average weight of 50 g were selected. Tanks were designed in the Marine and Environmental Research Institute of Jeju National University with the following parameters: 250 L capacity and flat bottom, aeration of sand-filtered seawater at a

salinity of $34 \pm 0.6\%$, and a temperature of $20 \pm 1^\circ\text{C}$. Abalones were pre-acclimatized for one week under the mentioned experimental conditions while feeding them with fresh marine seaweed (*Undaria pinnatifida*). Thirty animals were kept per tank.

2.6. Immune challenge experiment, RNA extraction, and cDNA synthesis

To conduct the immune challenge experiment, abalones were divided into five separate tanks. One group served as the unchallenged control group to analyze the tissue-specific distribution of *AbTrf* mRNA whereas another four groups were used for the challenged experiment. Each animal in first and second groups were injected intramuscularly with 100 μL of 1×10^4 CFU/mL live *V. parahaemolyticus* or *L. monocytogenes* bacteria, in saline solution. The third group was intramuscularly injected with 100 μL of LPS (5 $\mu\text{g}/\mu\text{L}$, *Escherichia coli* 055:B5; Sigma) in saline solution. Remaining group was injected with saline solution (0.9% NaCl), as an injection control. Different tissues including digestive tract, gill, female gonad (ovary), male gonad, hepatopancreas, mantle, and muscle were dissected from 4 unchallenged abalones. Hemolymph was collected from the pericardial cavities of abalones and centrifuged immediately at $3000 \times g$ for 10 min at 4°C to collect the hemocytes. The isolated tissues were immediately frozen in liquid nitrogen and transferred to -80°C for storage until further use. Each injected abalone group was randomly sampled at 3, 6, 12, 24, and 48 h post-challenge (at least four animals at each time point) and gill tissues along with hemocytes were isolated from each animal. Cells and tissues were immediately frozen in liquid nitrogen and transferred to -80°C for further storage until use for RNA extraction and cDNA preparation. Total RNA extraction was carried out using TRIzol[®] reagent (Sigma) according to manufacturer's protocol, diluted up to 1 $\mu\text{g}/\mu\text{L}$, and used to synthesize first-strand

cDNA using PrimeScript cDNA synthesis kit (TaKaRa Bio Inc.) according to the manufacturer's instructions. The cDNA was diluted 40-fold (800 μ L total volume) and stored at -20 $^{\circ}$ C until use.

2.7. Quantitative real time PCR (qPCR) analysis of mRNA expression levels

All the tissues extracted from normal and immune-challenged animals were quantitatively analyzed for the relative mRNA expression levels of *AbTrf* using quantitative real time PCR (qPCR). The DiceTM TP800 Real-Time Thermal Cycler System (TaKaRa, Japan) was used to carry out the qPCR reactions. The total volume of reaction mixture contained 4 μ L of diluted cDNA, 7.5 μ L of 2 \times TaKaRa Ex TaqTM SYBR premix, 0.6 μ L of sequence specific primers (Table 1), and 2.3 μ L of nuclease-free distilled H₂O. The thermal cycling conditions were as follows: 10 s at 95 $^{\circ}$ C, followed by 35 cycles of 5 s at 95 $^{\circ}$ C, 10 s at 58 $^{\circ}$ C, and 20 s at 72 $^{\circ}$ C with a final cycle of 15 s at 95 $^{\circ}$ C, 30 s at 60 $^{\circ}$ C, and 15 s at 95 $^{\circ}$ C. The DiceTM Real-Time System Software (version 2.0) automatically set the baseline. The Livak method (Livak and Schmittgen, 2001) was used to determine the mRNA expression of *AbTrf*. The same qPCR conditions were used to detect the internal control gene expression (ribosomal protein L5- GenBank ID: EF103443) using gene-specific primers (Table 1). The qPCR reactions were performed in triplicates and the data were presented as the mean \pm standard deviation (SD) of relative mRNA expression levels. The relative mRNA expression levels were normalized to 0 h time point (un-injected control) which was treated the baseline for comparison. Expression levels were further normalized to the corresponding saline-injected controls at each time point. Two-tailed un-paired *t*-test was used to determine whether the differences between experimental groups and un-injected control group were significant ($P < 0.05$).

2.8. Antibacterial assay for rAbTrf-N

In order to experimentally assess the antimicrobial activity of transferrin which is plausibly demonstrated via its iron-binding ability, two bacterial strains *E. coli* (iron dependent) and *L. plantarum* (iron independent) were used. As an iron-dependent bacterium, *Escherichia coli* was grown in LB broth at 37 °C for 6 h by shaking at 200 rpm. At the same time, as an iron-independent bacterium, *L. plantarum* was grown at 25 °C for 6 h by shaking at 200 rpm. The bacteria were harvested by centrifugation at 5000 × *g* for 10 min. The obtained *E. coli* and *L. plantarum* bacteria pellets were dissolved in LB broth. Subsequently, the cells were diluted to reach an initial density of 10⁵ cells/mL (absorbance approx. = 1.0) and 100 μL from each solution was added to the wells of 96-wells microtiter plate. Each well was supplemented with FeCl₃ (final concentration of 1 μM) to ensure the minimal Fe³⁺ amount required in the medium for microbial growth. To each well an aliquot of rAbTrf-N or MBP protein or elution buffer (controls) was then added to achieve the final concentrations of 150 and 300 μg/mL (final concentration of 2 and 4 μM) in the wells, respectively. The assay was carried out in triplicate to ensure the credibility of the results.

Table. 2: Oligomers used in this study (AbTrf)

| Name | purpose | Sequence (5' →3') |
|------------------|---|---|
| AbTrf- qF | qPCR of <i>AbTrf</i> | ATGGCGGAGAACTACCAGGACA |
| AbTrf- qR | qPCR of <i>AbTrf</i> | ACACCGTGTGGACGAGGACTTTAT |
| AbTrf- F | Amplification of coding region (<i>EcoRI</i>) | GAGAGAGaattcGAGGACGTAAATGCGCGGTTCT |
| AbTrf- R | Amplification of coding region (<i>HindIII</i>) | GAGAGAAagcttTTACTTGACGTAGTTTTCCAGCGTGTTCA |
| abRibI-F | qPCR for abalone RibI | TCACCAACAAGGACATCATTGTC |
| abRibI-R | qPCR for abalone RibI | CAGGAGGAGTCCAGTGCAGTATG |

3. Result and Discussion

3.1. Identification and bioinformatics characterization of *AbTrf* cDNA sequence and the derived amino acid sequence

The identified cDNA sequence for *AbTrf* (Accession No: KR052198) from the cDNA database was 4205 bp in length. It contained a 146 bp long 5'-UTR, 1875 bp long 3'-UTR, and 2184 bp long open reading frame encoding a 728 aa long protein sequence. The predicted molecular weight of the putative AbTrf protein was 80 kDa with an isoelectric point of 8.5. The molecular weights of the individual N-terminal and C-terminal domains were 35 kDa and 38 kDa, respectively. Using the SignalP online signal peptide predicting software, a 19 aa long 5'-signal peptide sequence was identified. According to the results obtained from the NCBI-CDD and ExPASy-prosite servers, the amino acid sequence also showed the typical and conserved features of transferrin proteins, including an N-terminal (24 aa–355 aa) and a C-terminal (360 aa–702 aa) (Fig. 2) transferrin signature domains, connected by a very short peptide span. Further revealed by NCBI-CDD, each individual domain contained the specific residues for the Fe³⁺ binding ability at the amino acid positions of D78, Y110, T136, G143 and D277 in N-domain and D415, Y444, T470, G477, and H621 in C- domain (Fig. 2). In addition to major active site amino acid residues, both N-terminal and C-terminal domains contained disulfide bond-forming cysteine residues which are known to be important in stabilizing protein structure for Fe³⁺ binding (Rose et al., 1986). According to the NCBI blast result, our putative AbTrf was aligned with melanotransferrin counterparts from other species, including human. Most of the active site amino acid residues of AbTrf were found to be conserved over invertebrates, fish, birds, and mammalian melanotransferrins (Fig. 2). In human

melanotransferrin, there are four distinguishable domains; N terminal signal peptide, N- terminal transferrin like domain, C- terminal transferrin like domain and hydrophobic GPI-anchor domain (Suryo Rahmanto et al., 2012). GPI anchor is essential for the melanotransferrin to be bound with cell membrane due its hydrophobic nature (Rose et al., 1986). The only features clearly identified in AbTrf were N- terminal signal peptide and two identical N- terminal and C- terminal transferrin like domains which have been identified as general features among transferrin family members including serotransferrin, lactoferrin and ovotransferrin. Extensive studies need to be conducted with AbTrf counterpart to identify the presence of GPI anchor region at 3' coding region of AbTrf, to investigate its membrane localization, and to examine whether it is a real orthologue of melanotransferrin.

Even though we could not identify in the AbTrf amino acid sequence, some studies on transferrins, such as those carried out in goldfish transferrin, have reported a cleavage site to cut and separate the two domains within the hinge region of N- and C-terminal domains (Sahoo et al., 2009). As previously reported, the cleaved-form participates in the mechanisms that lead to the activation of macrophages under pathological conditions. Hence, the lack of this feature in AbTrf may suggest the absence of such mechanism in abalones or bereft of the mechanism which leads to activate macrophages in abalones. However, to date, no study has investigated this aspect in mollusk biota; thus, extensive studies are required to decipher this putative phenomena.

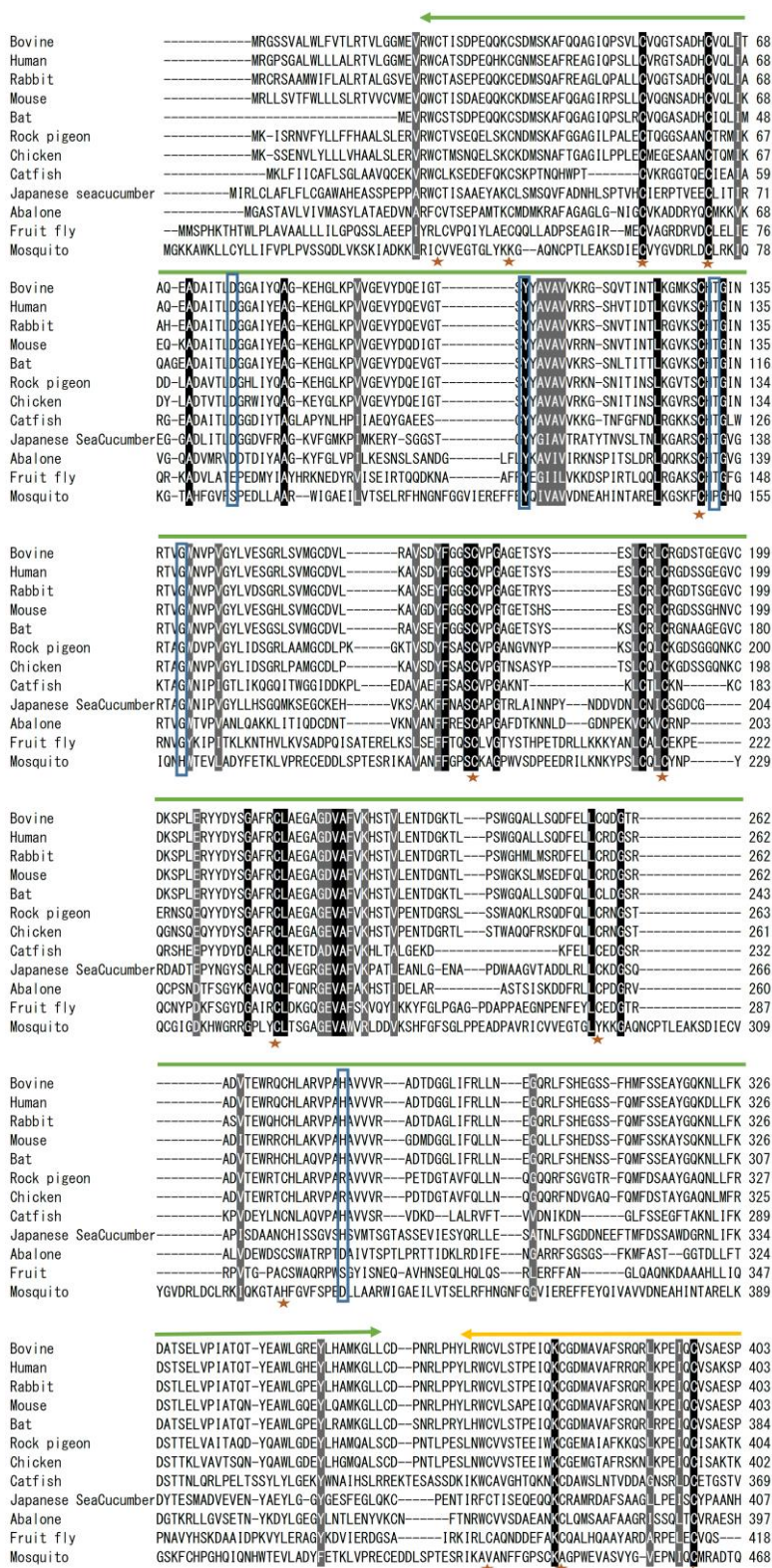


Fig 2:

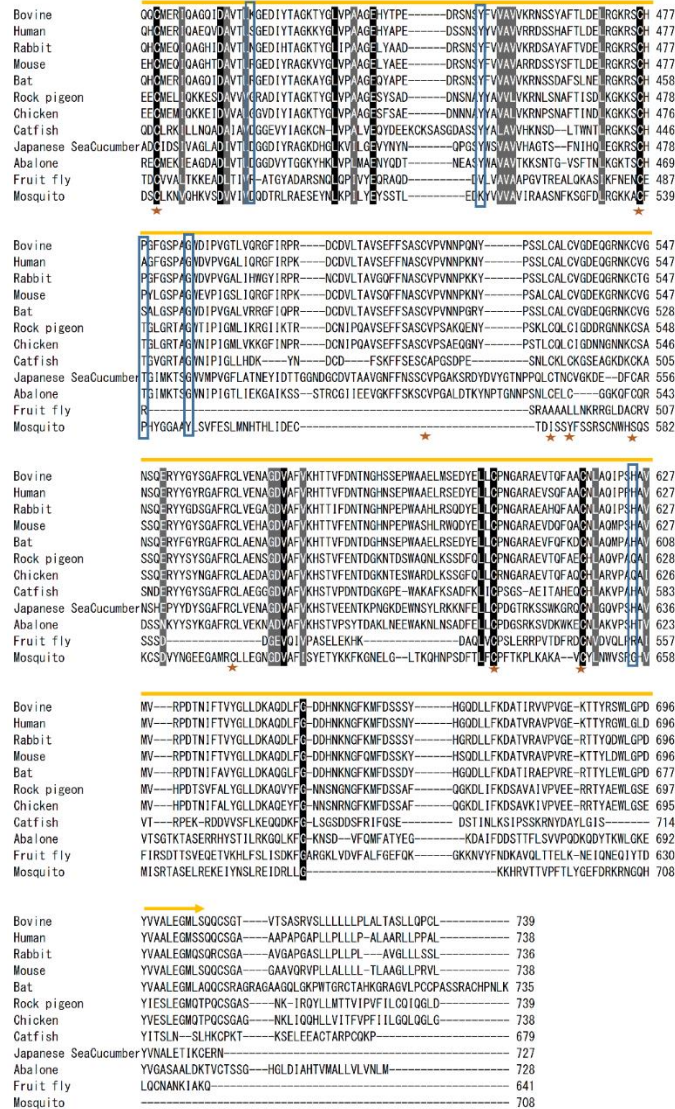


Fig 2: cont.

Figure 2: ClustalW multiple sequence alignment of the deduced amino acid sequences of AbTrf with known Trf proteins. The identical residues are highlighted in black color and semi conservative residues are highlighted in gray color. The N-terminal and C-terminal transferrin domains are indicated in green color and yellow color double-headed arrows, respectively. Active residues for iron binding are shown within blue color boxes. Highly conserved Cysteine residues are indicated in brown color stars.

3.2. Sequence homology and phylogenetic analysis of abalone transferrin amino acid sequence

As identified with human transferrin, there are 10 main amino acid residues important for iron binding (5 residues in each domain). 7 out of 10 amino acids important for iron binding were found to be identical with human transferrin (Fig. 2). This observation suggests that abalone transferrin may possess the similar type of potential structure to bind ferric ions (Lambert et al., 2005a). Moreover, the disulfide bond forming cysteine residues were found to be conserved over different species examined, ensuring the structural integrity of abalone transferrin that may be important for ferric binding (Fig. 2).

Table.3: Amino acid identity and similarity of AbTrf entire sequence to other homologs

| Species name | Common name | NCBI accession no. | a.a. (aa) | Identity | Similarity |
|--|-------------------------|--------------------|-----------|----------|------------|
| <i>Apostichopus japonicus</i> | Japanese sea cucumber | HQ260578.1 | 727 | 36.9% | 51.8% |
| <i>Columba livia</i> | rock pigeon | KB375824.1 | 739 | 37.1% | 54.3% |
| <i>Gallus gallus</i> | chicken | NM_205207.1 | 738 | 37.2% | 53.9% |
| <i>Bos taurus</i> | cattle | NM001192312.1 | 739 | 36.7% | 52.9% |
| <i>Myotis brandtii</i> | Brandt's bat | KE163428.1 | 735 | 34.5% | 50.9% |
| <i>Rattus norvegicus</i> | Norway rat | NM001105872.1 | 738 | 25.6% | 37.1% |
| <i>Homo sapiens(melanotransferrin)</i> | human | M12154.1 | 738 | 36.0% | 52.5% |
| <i>Mus musculus</i> | house mouse | NM013900.2 | 738 | 35.3% | 51.1% |
| <i>Oryctolagus cuniculus</i> | rabbit | NM001081992.1 | 736 | 36.5% | 52.9% |
| <i>Drosophila melanogaster</i> | fruit fly | AF061268.1 | 641 | 22.3% | 38.7% |
| <i>Culex quinquefasciatus</i> | southern house mosquito | XM001863377.1 | 708 | 21.5% | 34.0% |
| <i>Ictalurus punctatus</i> | channel catfish | FJ176741.1 | 679 | 34.0% | 49.2% |
| <i>Strongylocentrotus purpuratus</i> | Purple Sea Urchin | XP_786179 | 768 | 39.2% | 54.0% |

In order to draw an overall picture on the evolutionary position of AbTrf with other studied transferrins to date from different organisms, AbTrf amino acid sequence was compared in pairwise manner with transferrins from different species. The pairwise-comparison analysis of AbTrf putative amino acid sequence with other available peptide sequences (Table 3) showed that AbTrf exhibited 39.2% of identity and 54.0% of similarity with *Strongylocentrotus purpuratus* transferrin. Similarly, AbTrf exhibited 36.0% of identity and 52.5% of similarity with human transferrin. Even though, the identity and similarity level is lower, these observations suggested that the amino acid sequence of AbTrf has similar levels of homology to both invertebrate and mammalian counterparts. To further investigate the evolutionary development of AbTrf, the phylogenetic tree was constructed adopting the neighbor-joining method supported by bootstrap analysis (5000 bootstrap replicates). In the phylogenetic tree, vertebrates such as birds, mammals and fish have been clustered together. Moreover, birds and mammals have shared a common ancestor while fish exhibited a separate clade with a different ancestor. With relevant to invertebrates, deuterostomes such as *Strongylocentrotus purpuratus* and *Apostichopus japonicas* along with disk abalone have clustered together while exhibiting a closer evolutionary relationship with other vertebrates, even though invertebrate protostomes such as *Drosophila melanogaster* and *Culiseta longiareolata* located as evolutionarily distance out groups (Fig. 3). These observations may conclude the presence of two invertebrate transferrins, one of them is closer to vertebrate counterparts and the other is distant from vertebrates. More transferrin counterparts from invertebrates need to be identified and annotated, in order to confirm this putative evolutionary relationship.

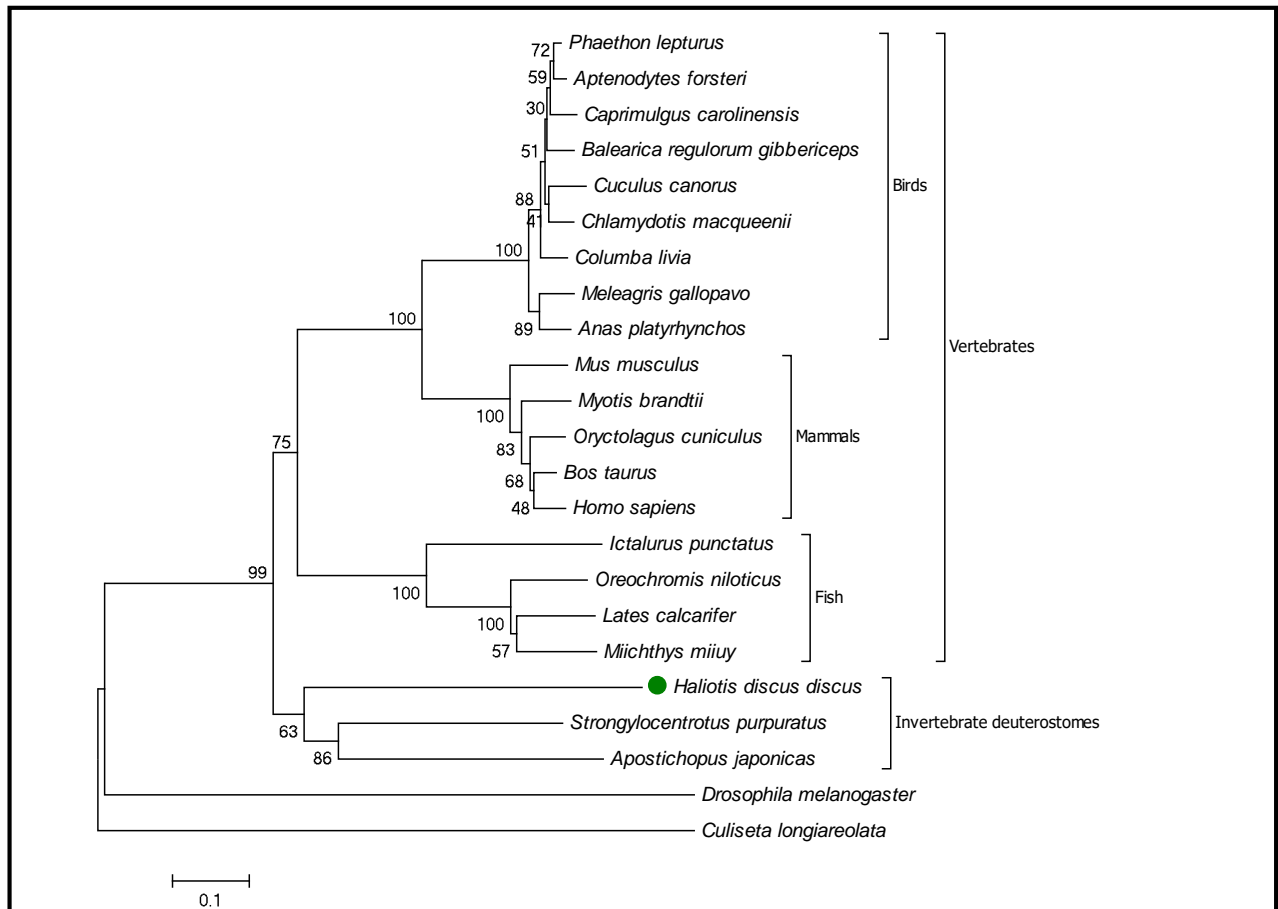


Figure 3: Phylogenetic analysis of AbTrf with selected known full-length Trf amino acid sequences of other species. Branch numbers are the bootstrap values for 5000 replicates. Location of abalone homolog is indicated with a green color circle. Different clusters are indicated separately between parentheses. The NCBI-GenBank accession numbers of the amino acid sequences of the organisms used in the comparison are mentioned in Table 2 except: *Haliotis discus discus* - KR052198, *Phaethon lepturus*- XP_010280026, *Aptenodytes forsteri*- XP_009280606, *Caprimulgus carolinensis*- XP_010169327, *Balearica regulorum gibbericeps*- XP_010302177, *Cuculus canorus*- XP_009563890, *Chlamydotis macqueenii*- XP_010117825.1, *Meleagris gallopavo*- XP_003209160.1, *Anas platyrhynchos*- XP_005014405.1, *Lates calcarifer*- AEZ51816, *Miichthys miiuy*- AFC68982.1, and *Oreochromis niloticus*- ABB70391.1.

3.3. Putative functional prediction of AbTrf based on the construction of the 3D structure

In order to predict the locations and orientations of functionally important residues of AbTrf in Fe^{3+} binding at its structural level, a three dimensional (3D) structure of AbTrf was obtained and annotated by applying a homology-based modeling using the online SWISS-MODEL server. To generate the 3D structure, crystalized full-length apo-human transferrin (hTF) resolved to 2.6 Å resolution was used as template (Noinaj et al., 2012). This protein shared 41.69 % of sequence identity with the putative AbTrf amino acid sequence.

In the tertiary structure, two N-terminal and C-terminal putative transferrin-like globular domains linked by the putative hinge region were clearly observed (Fig. 4). Each active site possessed the putative amino acid residues that are believed to be essential in Fe^{3+} binding. The active residues involved in iron binding were oriented and gathered in the hydrophilic cavity of the pictured putative AbTrf 3D structure which showed analogy with the canonical tertiary structure of typical transferrin (Lambert et al., 2005a). The two domains may host two Fe^{3+} molecules in their putative iron-binding cavities. Thus, the tertiary structure of AbTrf holds most of the key features of the transferrin family that are necessary to be categorized as a true transferrin homolog.

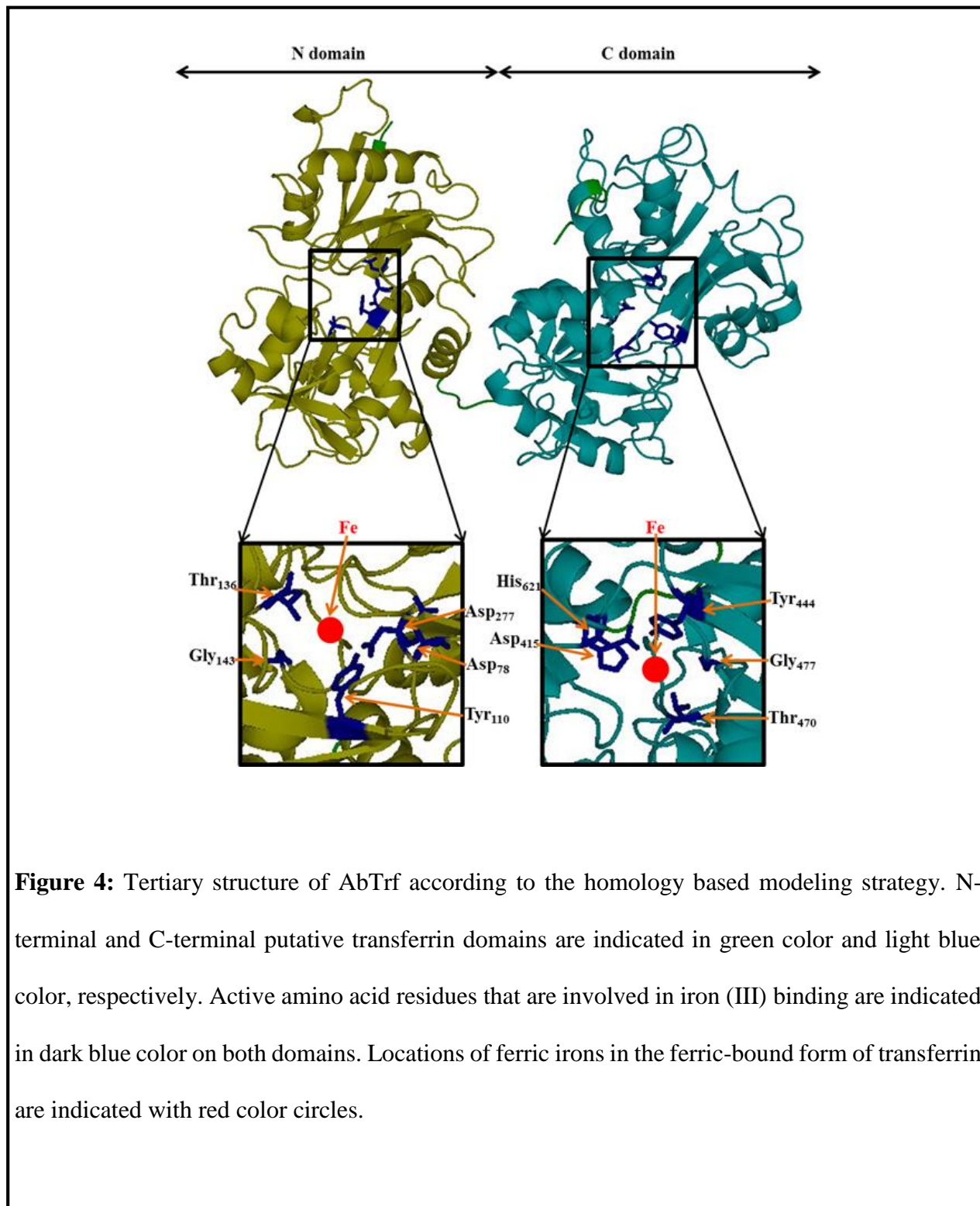


Figure 4: Tertiary structure of AbTrf according to the homology based modeling strategy. N-terminal and C-terminal putative transferrin domains are indicated in green color and light blue color, respectively. Active amino acid residues that are involved in iron (III) binding are indicated in dark blue color on both domains. Locations of ferric irons in the ferric-bound form of transferrin are indicated with red color circles.

Even though the currently identified putative AbTrf sequence exhibited the bilobed nature of typical mammalian transferrins, most of the previously reported invertebrate transferrin-like molecules bear different types of domain architectures. Most of the invertebrate transferrins show a great diversity with respect to the number of lobes and the iron-binding ability of their domains. In recent study, in amphioxus *Branchiostoma belcheri* (*B. belcheri*), a bilobed transferrin was identified. Although it contains two lobes at the N-terminal and C-terminal, the C-terminal domain was found to contain a long intervening sequence that might replace the loss of Fe³⁺ binding functionality of the C-terminal domain (Liu et al., 2009). Protein structures with two as well with one lobe have been identified from urochordates (Abe et al., 2001). In marine algae, a species with a three lobed structure has also been reported (Fisher et al., 1997; Fisher et al., 1998; Schwarz et al., 2003).

3.4. Functional assessment of the putative AbTrf-N protein in Fe³⁺ binding using purified recombinant AbTrf-N protein

To experimentally investigate and demonstrate the functional nature of AbTrf, recombinant N-terminal transferrin domain was expressed in *E. coli* and purified by maltose affinity chromatography. The purified recombinant protein was visualized on SDS-PAGE and a single band was observed corresponding to the pure form of the purified protein with a molecular weight of ~78 kDa, confirming the theoretically predicted molecular weight of its N-terminal domain (36 kDa) since MBP is around 42.5 kDa (Fig. 5). After elution of the purified AbTrf-N, in order to identify the putative Fe³⁺ binding ability of AbTrf, the recombinant AbTrf N-terminal domain was assayed using the standard chrome azurol S (CAS) assay reagent.

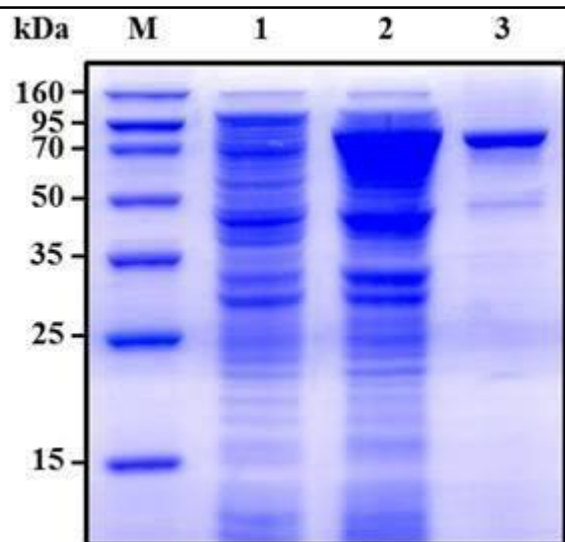


Figure 5: SDS-PAGE analysis of rAbTrf-N protein. Columns represent: protein marker (M), total cellular extract before IPTG induction (1), recombinant protein in supernatant (crude protein) (2), and eluted AbTrf-MBP protein after purification (3).

The method originally was proposed for siderophores detection by Bernhard Schwyn and J. B. Neilands (Schwyn and Neilands, 1987). Once the purified rAbTrf-N was incubated with the CAS assay solution, the color of the mixture changed from blue to yellow indicating the iron-binding ability of AbTrf. Further, the color change exhibited a dramatic increase in intensity with increasing protein concentration which in turn reduces the OD_{630} ratio (between the negative control and test samples, 1 hour after incubation with the proteins) (Fig. 6). According to the general principle, dye- Fe^{3+} complexes are purple and dye without Fe^{3+} is yellow. Therefore, binding of iron by transferrin will result in a dose-dependent change in color.

This assay has previously been used to determine the iron-binding ability of the transferrin-like protein from *B. belcheri* (Liu et al., 2009) as well as in studies assessing the iron requirement of *L. plantarum* species (Pandey et al., 1994).

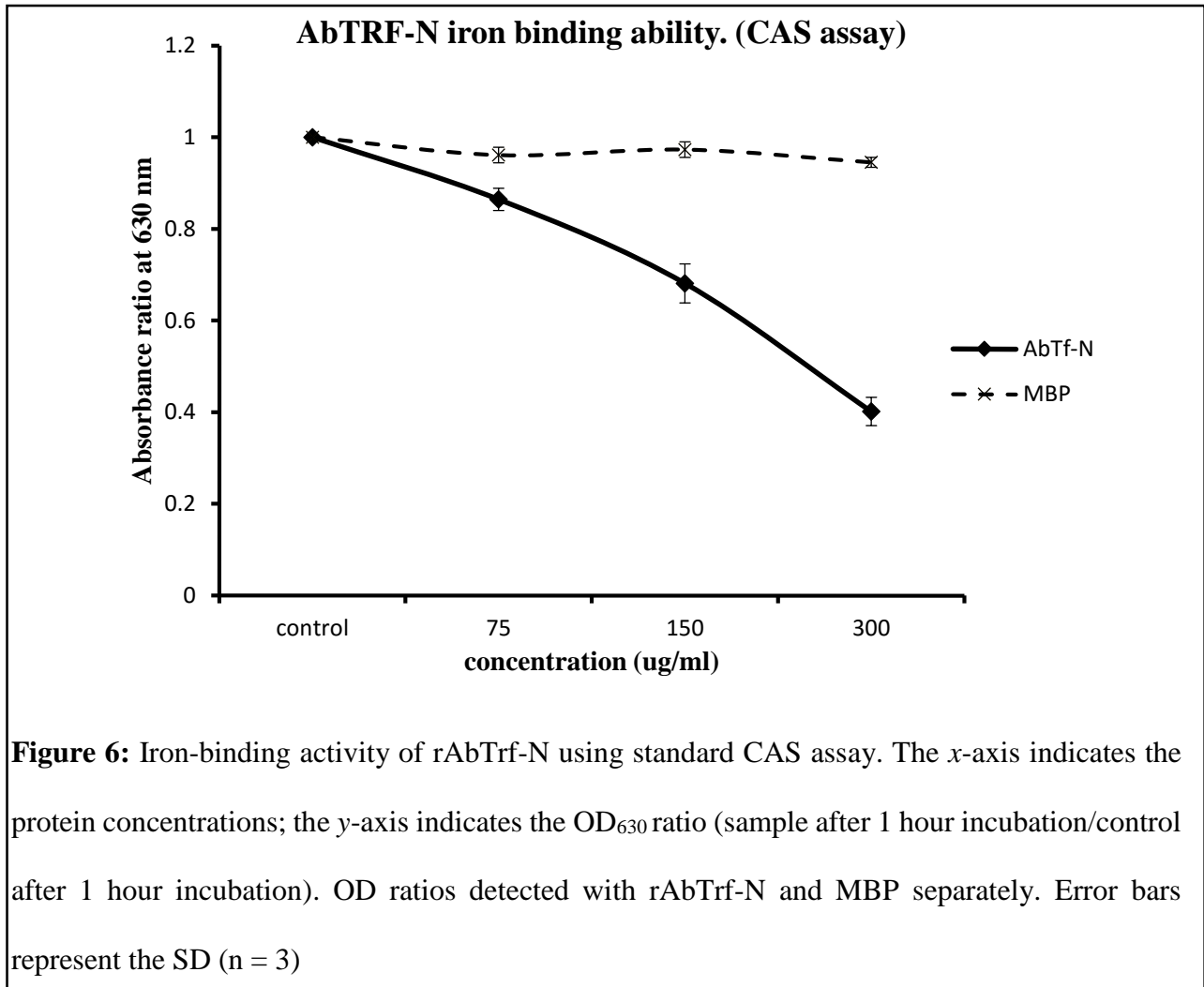


Figure 6: Iron-binding activity of rAbTrf-N using standard CAS assay. The *x*-axis indicates the protein concentrations; the *y*-axis indicates the OD₆₃₀ ratio (sample after 1 hour incubation/control after 1 hour incubation). OD ratios detected with rAbTrf-N and MBP separately. Error bars represent the SD (n = 3)

3.5. Tissue specific expression of *AbTrf* mRNA

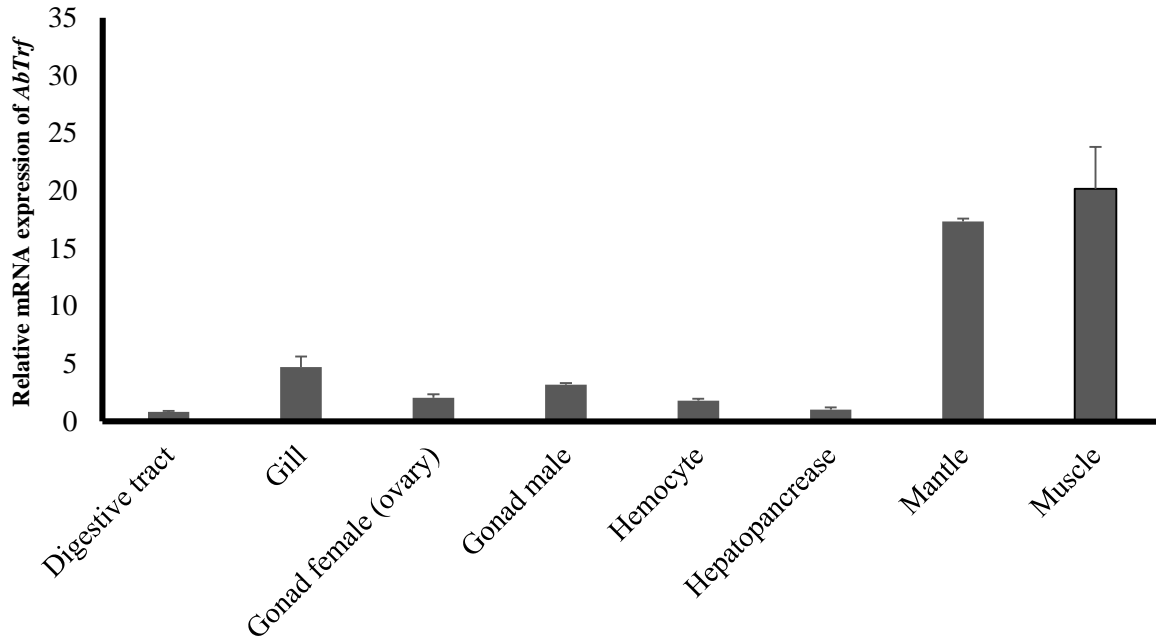


Figure 7: Tissue specific mRNA expressions of *AbTrf* determined by qPCR. Fold mRNA expression of *AbTrf* in different tissues relative to that of hepatopancreas tissue under physiological conditions is indicated. Error bars represent the SD (n = 3).

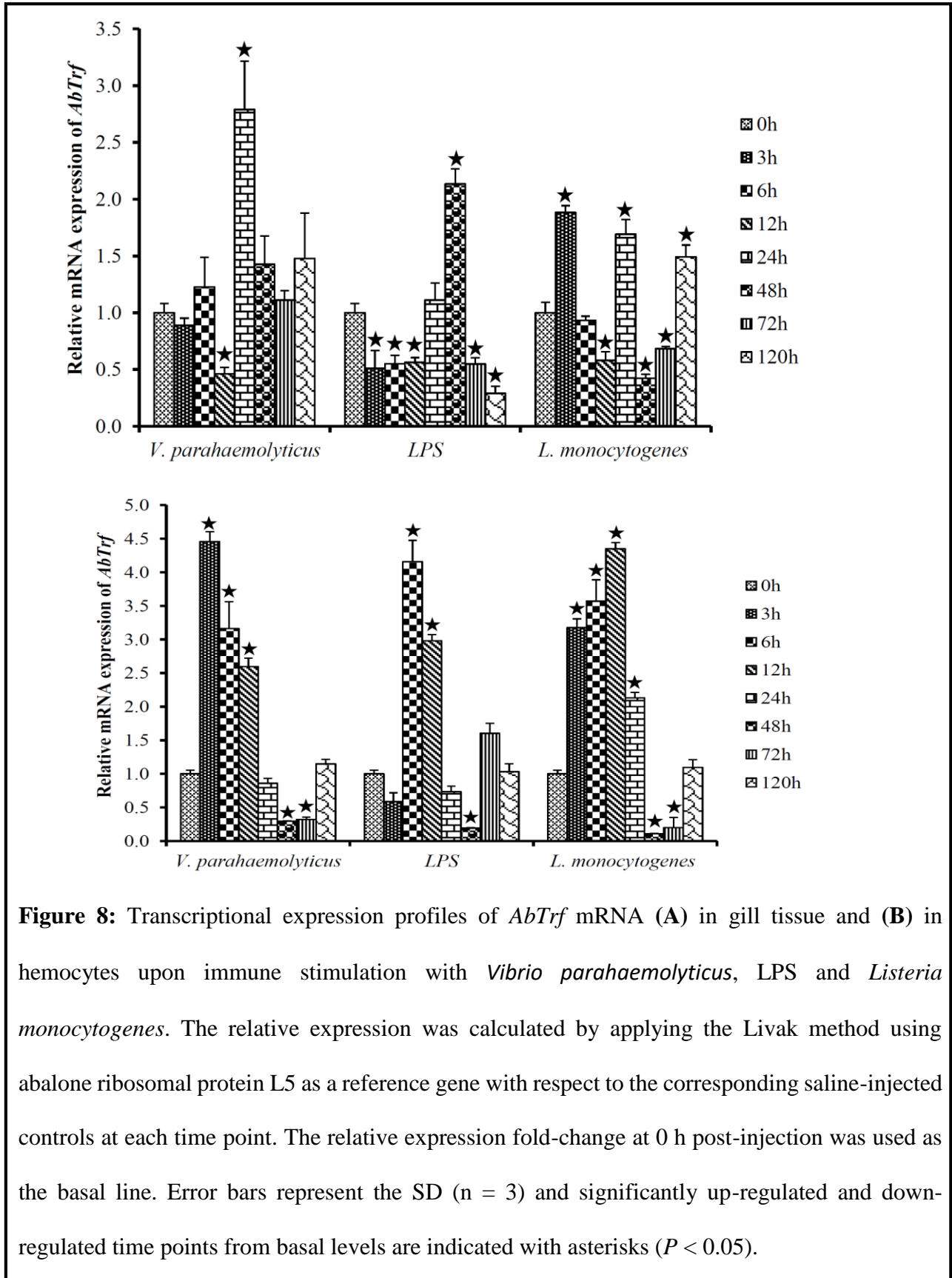
To gain the preliminary insight to check whether transferrin has any antimicrobial responses, we investigated the tissue specific basal mRNA expressional levels of *AbTrf* gene. Tissue specific mRNA expression levels were quantified to examine the basal level of *AbTrf* mRNA expression in different tissues. The highest mRNA expression levels were detected in muscle and mantle. In overall, mRNA expression was shown to be ubiquitously dispersed among all the other examined tissue types (Fig. 7). In most vertebrates, transferrin transcripts have been detected at high levels

in liver tissue, since it is the primary site for transferrin synthesis (Beutler et al., 2000). Regarding invertebrates, *B. belcheri* exhibited the highest expression levels in hepatic caecum (Liu et al., 2009). In crustaceans, expression of transferrin-like transcripts was detected at high levels in the hepatopancreas (Toe et al., 2012). Muscle and mantle tissues are highly susceptible to the marine pathogens since these tissues are frequently in contact with outer environment. Hence, compared to the other organisms, there is a high possibility to detect pronouncedly expressed innate immunological counterparts in outer layers of marine gastropods such as abalones. However in mollusk, no reports are available to date on transferrin or transferrin-like transcript expression. The results from the present study may predict a wide role of transferrin in molluscan physiology since its transcripts were detected in a diverse range of tissues.

3.6. Modulation of *AbTrf* mRNA profile upon pathogenic challenge conditions

Since transferrin is a major acute-phase protein that can act as a potent antimicrobial agent in most inflammatory conditions, its mRNA expression levels were examined in different tissue types in response to different pathological conditions. High expression levels of *AbTrf* were found in immunologically important tissues, the gill and in hemocytes, which are known to play a role in immunity against the common bacterial infectious agents *V. parahaemolyticus*, *Listeria monocytogenes* and the well-known bacterial endotoxin LPS. *V. parahaemolyticus* is known to be a common shellfish pathogen of abalone species (Elston and Wood, 1983; Lee et al., 2003). On the other hand, shellfish were found to be frequently contaminated with *Listeria monocytogenes*. Thus, we used these pathogens for our time course immune challenge experiment.

Upon the injection, significantly elevated mRNA expression levels were detected in the gill tissue at 24 h post injection (p.i.) with *V. parahaemolyticus*, at 3 h and 24 h p.i. with *Listeria monocytogenes* and 48 h p.i. with LPS (Fig. 8A). After the fish were treated with all three immune stimulants, intense *AbTrf* expressional stimulations were observed with significantly high mRNA levels at 3 h, 6 h, and 12 h p.i. with *V. parahaemolyticus*, 3 h, 6 h, 12 h and 24 h p.i. with *L. monocytogenes* and 6 h and 12 h p.i. with LPS (Fig. 8B).



In brief, a potent induction of *AbTrf* upon pathogenic challenge conditions was observed in this experiment. Moreover, *AbTrf* was detected more promptly in hemocytes than in the gill tissue. In both tissues, more intense responses were detected upon *V. parahaemolyticus* and *L. monocytogenes* treatments (whole bacteria), than LPS (pathogen mimic) treatment.

To date, the transcription of the *Trf* gene has been modulated upon different pathological conditions in a wide range of species, which led to the investigation of its immune response under inflammatory conditions. In mammals, transferrin expression has been investigated in species such as rabbit and rat (Schreiber et al., 1979). Fish such as Chinese black sleeper (*Bostrichthys sinensis*) show high expression levels of transferrin transcripts in both embryonic and other development stages under pathological conditions (Gao et al., 2013). Transferrin from insects has also been shown to be expressed under pathological conditions (Guz et al., 2007; Yoshiga et al., 1999; Yoshiga et al., 1997; Yun et al., 1999). Overall, the expression patterns observed against common immune stimulants have suggested the possible involvement of *AbTrf* in early-phase host defensive mechanisms, which is in accordance with the detected anti-bacterial activity of rAbTrf.

3.7. Investigation of antimicrobial property of AbTrf-N

To date, several studies have been conducted on mammals (Schreiber et al., 1979), fish (Bayne et al., 2001), and insects (Ong et al., 2006), in order to assess the antimicrobial property of transferrin generated due to its binding to Fe^{3+} . However, the present study is the first molecular characterization of a transferrin-like protein in invertebrate mollusk biota and, thus, it provides novel information regarding the antimicrobial property of invertebrate transferrin-like proteins due

to their iron-binding ability. Few studies have assessed the iron-binding ability of invertebrate transferrin-like proteins but they did not correlate this with their antimicrobial property.

As mentioned above, we have observed that AbTrf-N has the general iron binding property and AbTrf is expressed under common pathogenic challenged conditions. Due to these observations, we speculated some immunological functions of abalone transferrin as well. Therefore, in order to understand the antimicrobial properties of AbTrf-N mediated by its Fe³⁺ depriving ability, experiments were designed and conducted as described in the methodology section. In the experimental study, two bacterial species *E. coli* and *L. plantarum*, which are iron dependent and iron independent, respectively, were used to analyze their growth and propagation. The rAbTrf-N exhibited detectable antibacterial effect against *E. coli* DH5 α by significantly (two-tailed un-paired t-test, $P < 0.05$) inhibiting its growth in the culture medium from 2 h post incubation in a dose-dependent manner (Fig. 9A). *L. plantarum* was used as the negative control and did not exhibit any delay in the growth rate compared to the control (Fig. 9B). Similarly, its growth rate did not show any dose dependent changes despite the changes in rAbTrf-N concentration. The growth curves were synchronized and showed impacts on each other, irrespective to the dose of added protein.

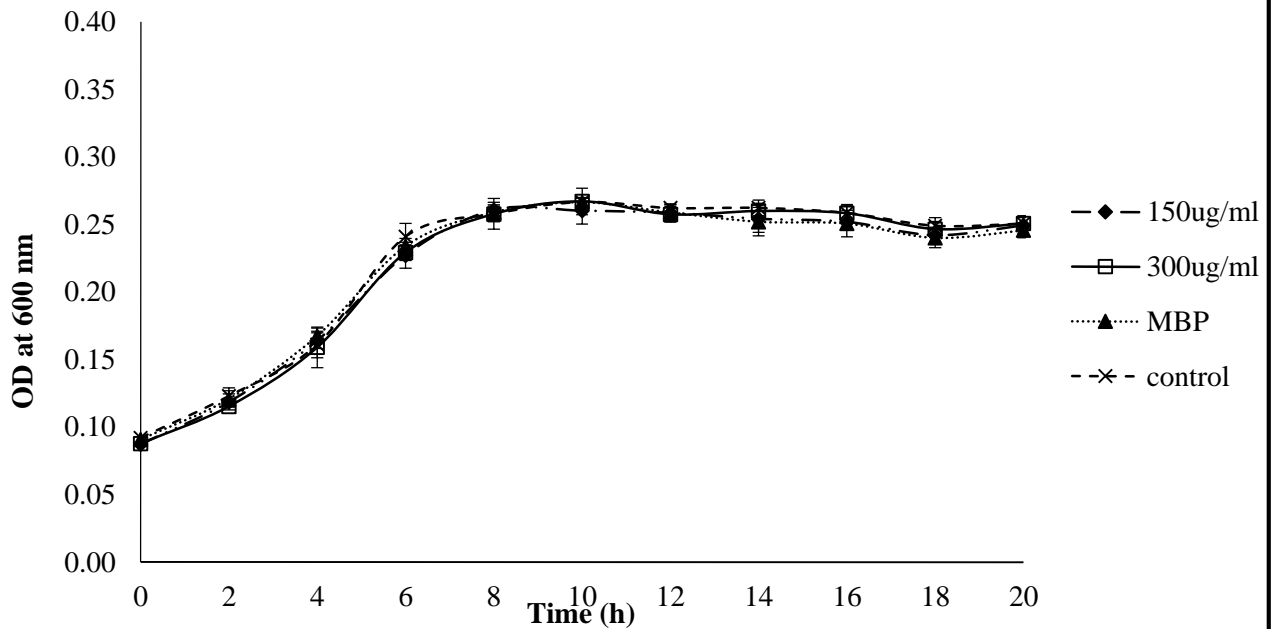
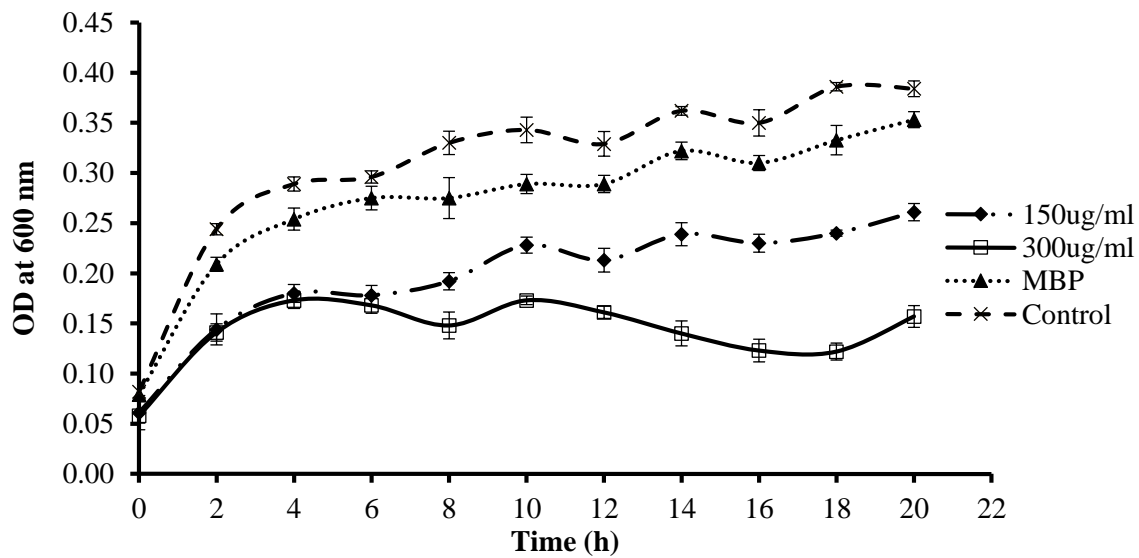


Figure 9: The bacteriostatic activity of rAbTrf. (A) The growth curve of *E. coli*. (B) The growth curve of *Lactobacillus plantarum*. The *x*-axis indicates time; the *y*-axis indicates the OD at 600 nm. Each point in the graph represents the mean of at least three assays.

Iron is an essential nutrient to be acquired by almost all the animals including macro- and micro-organisms due to its involvement in a number of key cellular biological processes such as oxygen transport, ATP generation, cell growth and proliferation, and detoxification. In most microbes, iron acts as a co-enzyme and works collaboratively with ribonucleotide reductase in order to catalyze a key step in the DNA synthesizing process (Thelander et al., 1983). Due to these reasons, depletion of Fe^{3+} molecules from biological fluids by its binding with proteins such as transferrin has a great effect on the growth of invader pathogens under pathological conditions. Since AbTrf was able to inhibit the growth of *E. coli*, transferrin from abalone may show an antimicrobial activity against iron requiring bacterial species similar to the mechanism identified in most vertebrate and mammal transferrins. Previous studies have experimentally proven that *E. coli* is iron dependent for growth-related metabolic processes while LAB strains such as *L. plantarum* are iron independent for growth-related metabolic processes. According to previous studies conducted on lactic acid bacteria (LAB), most *Lactobacillus* species have been shown to be iron independent for growth and the above discussed metabolic processes (Bruyneel et al., 1989). Moreover, it has been experimentally proven using CAS assay and radiolabeled Fe molecules that LAB species including *L. plantarum* do not produce siderophore or manipulate iron. Due to this reason, their growth rates were not affected by either the changes in iron concentration in the medium or the addition of synthetic iron chelators for growth inhibition purposes (Archibald, 1983; Pandey et al., 1994). Based on these findings, we designed our experimental study by manipulating *L. plantarum* in order to investigate the antimicrobial properties exhibited by transferrin due to its binding to Fe^{3+} .

To our knowledge, this is the first report in mollusk biota showing *in vivo* the antimicrobial property of transferrin via its Fe³⁺ binding ability. In addition, the present study provides novel insights and ways to investigate how iron scavengers such as transferrin affect the growth of two different microbial model systems which are iron dependent (*E. coli*) and independent (*L. plantarum*) for their growth.

In conclusion, we identified a transferrin homolog (AbTrf) from disk abalone and characterized it at the molecular, expressional, and functional levels. This is the first characterization of this sort in molluscan taxa. The putative *AbTrf* cDNA sequence bears the typical two identical homologous domains of the transferrin family. The mRNA expression levels were investigated under physiologically normal and pathological conditions. *AbTrf* exhibited a ubiquitous tissue expression profile while showing intense responses under pathological conditions. The positive results obtained in the standard CAS assay using the recombinant AbTrf N-terminal domain suggest its putative iron-binding activity. The antimicrobial activity was assessed against two bacterial species *E. coli* (BL21) and *L. plantarum*, and we observed that AbTrf inhibited the growth of *E. coli* significantly, while no effect was observed on the growth rate of *L. plantarum*, suggesting the iron deprivation is one of the mechanism functioning behind the detected antimicrobial activity of AbTrf. Taken together, our study extends the current knowledge on transferrin in the invertebrate molluscan family, as well as demonstrates the homologous functional behavior of AbTrf to its mammalian counterparts in terms of its antimicrobial activity.

CHAPTER II:

Molecular identification and functional delineation of a glutathione reductase similitude from Disk abalone (*Haliotis discus discus*): insights as a potent player in host antioxidant defense

1. Abstract

Glutathione reductase (GSR) as an enzyme catalyzes the biochemical conversion of glutathione oxidized form (GSSG) into reduced form (GSH). Since ratio between two forms of glutathione (GSH/GSSG) is important for the proper functionality of GSH to act as an antioxidant against H_2O_2 , contribution of GSR is essential. Abalones are marine molluscans which frequently encounter environmental factors which can trigger the overproduction of ROS such as H_2O_2 . Therefore, we conducted the current study to reveal the molecular and functional properties of GSR similitude identified from disk abalones (*Haliotis discus discus*). The identified cDNA sequence (2325 bp) bears a 1356 bp long ORF, coding for a 909 bp long amino acid sequence which harbored a pyridine nucleotide – disulphide oxidoreductase domain (171-246 aa), a Pyridine nucleotide-disulphide oxidoreductase dimerization domain and a Rossmann-fold NAD(P)(+)-binding proteins superfamily signature. Four functional residues; FAD binding site, glutathione binding site, NADPH binding motif and assembly domain were identified to be conserved among the other species. The recombinant AbGSR (rAbGSR) exhibited a detectable activity with standard glutathione reductase activity assay. The optimum pH and optimum temperature for the reaction were detected at 7.0 pH and 50 °C, respectively while showing no effect of the ionic strength of the medium. The enzymatic reaction was vastly inhibited by Cu^{+2} and Cd^{+2} ions. A considerable cell protective effect was detected with disk diffusion assay conducted with rAbGSR.

Moreover, with MTT assay and flowcytometry, significance of cell protectiveness provided by rAbGSR was confirmed. Moreover, *AbGSR* was found to be ubiquitously distributed in different types of abalone tissues. *AbGSR* mRNA expression exhibited the potent inductions in three immune challenges conducted with *Vibrio parahaemolyticus*, *Listeria monocytogenes* and LPS predicting its possible involvements in host defense mechanisms under pathogenic infections. Taken together, results of current study suggest that AbGSR might play an important role in antioxidant mediated host defense mechanisms while providing insights into immunological contribution of AbGSR.

Keywords: Glutathione reductase, abalone, antioxidant activity, biochemical properties, transcriptional analysis

2. Material and Methodology

2.1. Identification of *AbGSR* cDNA from cDNA database

The cDNA sequence corresponding to *AbGSR* was identified from our previously established abalone transcriptome database (Lee et al., 2011) using the Basic Local Alignment Search Tool (BLAST) (<http://blast.ncbi.nlm.nih.gov/Blast.cgi>). Then, the identified abalone glutathione reductase similitude was designated as *AbGSR*.

2.2. Sequence characterization, evolutionary relationships and structural prediction of AbGSR

The location of open reading frame (ORF) of putative *AbGSR* on the identified cDNA sequence and physiochemical properties of putative amino acid sequence were predicted using DNAsist 2.2 program (version 3.0). The homologous protein sequences for AbGSR were identified using NCBI-BLAST search tool (<http://blast.ncbi.nlm.nih.gov/Blast.cgi>). Pairwise sequence comparisons with other relative organisms were conducted using EMBOSS needle (https://www.ebi.ac.uk/Tools/psa/emboss_needle/) server, and multiple sequence alignment was generated by using ClustalW2 program (Thompson et al., 1994). The phylogenetic tree that display the evolutionary relationship of AbGSR with other organisms was constructed by using the Molecular Evolutionary Genetics Analysis (MEGA) software version 6 (Tamura et al., 2013), implementing the Neighbor-Joining method supported by bootstrapping values taken from 5000 replicates.

The specific signature domains to represent glutathione reductase family were identified and located on amino acid sequence using ExPASy-prosite server (<http://prosite.expasy.org>) and the NCBI conserved domain database (CDD) (Marchler-Bauer et al., 2011). The corresponding tertiary structure of putative AbGSR amino acid sequence was generated using online protein structure modeling interface; SWISS model (Arnold et al., 2006) and visualized by using PyMOL molecular graphic software version 1.3 (Warren) for further structural annotation. In this regard, a 1.80 Å resolution crystal structure of human glutathione reductase (PDB no. 3DJG) was selected from the PDB database and used as the template for AbGSR.

2.3 Recombinant expression and purification of putative AbGSR protein

Two sequence specific forward and reverse primers were designed with NdeI and EcoRI restriction sites, respectively incorporated to 5' ends to amplify the cDNA region corresponding to the mature AbGSR peptide. The PCR reaction was conducted in a 50 μ L reaction mixture by adding 5 μ L of 10 \times Ex Taq Buffer, 4 μ L of 2.5 mM dNTPs, 40 pmol of each primer, 50 ng of hemocytes cDNA and 5 U of Ex Taq polymerase (TaKaRa) and adjusting PCR condition as follows ; Initial denaturation 94 $^{\circ}$ C for 3 min, there after 35 cycles of amplification at 94 $^{\circ}$ C for 30 s, 59 $^{\circ}$ C for 30 s and 72 $^{\circ}$ C for 1.5 min; and a final extension at 72 $^{\circ}$ C for 5 min. Subsequently, resulted PCR product was run on an agarose gel, and purified using AccuprepTM gel purification kit (Bioneer-Korea).

The recombinant prokaryotic AbGSR expression system was designed by manipulating with pMALTM-C5X prokaryotic expression vector (New England Biolabs, Ipswich, MA, USA). Both pMALTM-C5X vector and gel purified PCR product were simultaneously digested with NdeI and EcoRI endonucleases. Then digested PCR fragment was inserted into vector by ligating with Mighty Mix DNA Ligation Kit (TaKaRa). The accuracy of recombinant construct (pMAL-C5X/AbGSR) was confirmed by sequencing the insert of the vector construction at Macrogen-Korea. A sequence confirmed single clone was selected and transformed into *Escherichia coli* ER2523 competent cells (Novagen).

The pMAL-C5X/AbGSR transformed ER2523 cells were cultured in LB rich medium supplemented with 100 μ g mL⁻¹ ampicillin and 100 mM glucose incubated at 37 $^{\circ}$ C until OD₆₀₀ reached \sim 0.3. Then, temperature was adjusted to 20 $^{\circ}$ C in order to perform the protein induction. Once the OD₆₀₀ reached \sim 0.5, Protein induction was performed by adding isopropyl- β -

thiogalactopyranoside (IPTG) to the culture medium at a final concentration of 0.5 mM while maintaining the temperature at 20 °C. The culture was further incubated for 12 h at 20 °C and then cells were harvested by centrifugation at 3500 rpm for 30 min at 4 °C. The cell pellet was resuspended in column buffer (20 mM Tris-HCl, pH 7.4, 200 mM NaCl) and stored overnight at -20 °C. Following day, the cell suspension was thawed and then it was sonicated on ice in the presence of lysozyme (1 mg mL⁻¹). The resultant cell lysate was centrifuged at 9000 × g for 30 min at 4 °C. The supernatant was carefully pipetted and loaded into a column packed with amylose resin, and allowed to pass through the resin with gravity flow. The resin bound with protein was washed with 10 × volume of the column buffer. Finally, protein was eluted by adding elution buffer (column buffer + 10 mM maltose). The protein purification method was monitored in stepwise manner by collecting the sample fractions at different steps of purification procedure and loading them into a 12% SDS-PAGE gel along with standard molecular-weight size marker (PageRuler Plus, Thermo Scientific) and stained with 0.05% Coomassie blue R-250. The protein concentration was measured by the Bradford protein assay (Bradford, 1976). To overexpress the maltose binding protein (MBP), aforementioned protocol was repeated with pMAL-C5X vector instead of pMAL-C5X/AbGSR vector construction.

2.4. GSR specific enzymatic assay, assessment of enzymatic properties of rAbGSR and inhibitory effect of metal ions

2.4.1. Glutathione reductase activity assay

The activity of rAbGSR was assayed using the Glutathione Reductase Activity Colorimetric Assay Kit (BioVision, USA). Activity was measured to mU/mL following the protocol provided by manufactures. In brief, concentration series of rAbGSR and MBP were prepared as, 1.0, 0.5, 0.25 and 0.1 ng/ μ L. Fifty microliters of each protein was mixed with 50 μ L of reaction mixture (40 μ L of GR assay buffer, 2 μ L of 5, 5'-Dithiobis (2-nitrobenzoic acid) solution, 2 μ L of NADPH-GNERAT™ solution and 2 μ L of GSSG solution) as per protocol. Each experiment was carried out at triplicated on 96 well plates, and absorbance was measured by using multiplate reader (Multiskan EX, Thermo Scientific). The absorbance reading 1 (A_1) was measured at 405 nm immediate after mixing while measuring absorbance reading 2 (A_2) after 10 minutes incubation at 25 °C. As per protocol, the GSR activity was calculated using absorbance differences ($\Delta A_{405nm} = A_1 - A_2$) for each concentrations. Finally, the specific activity was determined after plotting a line chart showing GSR activity with respect to the concentration.

2.4.2. Enzymatic properties determination

A gradient of pH buffers was prepared ranging from 4.0 to 9.0 in order to assess the optimal pH for the activity of AbGSR. The above enzymatic reaction was conducted at different pH levels, and absorbance differences (ΔA_{405nm}) were obtained. To prepare buffering solutions, acetic acid (pH 3, 4, 5) phosphate (pH 6, 7, 8), and glycine - NaOH (pH 9) were used. To determine the optimum temperature, enzymatic assay was carried out at different temperature points of 10, 20,

30, 40, 50, 60 and 70 °C respectively. The optimum ionic strength was determined by conducting the enzymatic activity assay in different concentrations of tris HCl ranging 1000, 500, 250, 100, 10, and 0 mM at the pH 7.0. In each reaction, the average $\Delta A_{405\text{nm}}$ was calculated.

2.4.3. Effect of heavy metals on rAbGSR activity

In order to investigate the interference of metal ions on the enzymatic activity of rAbGSR, concentration gradients of heavy metal ions [(Cu⁺² - 0-2 mM) (Cd⁺² - 0-10 mM)] were prepared and the reaction was conducted in the mediums with heavy metals. To prepare metal ion gradients, CuSO₄.5H₂O from Duksan Pure Chemicals (Cu⁺²) and cadmium chloride hemi (penta hydrate) from sigma (Cd⁺²) were used. Subsequently, enzymatic activity was measured. Another experiment was conducted without adding the metal ions to treat it as the control with 100 % activity. The graph between activity and metal ion concentration was plotted and IC₅₀ values were obtained using corresponding graphs.

2.5. Antioxidant properties of rAbGSR

2.5.1. Disk diffusion assay

The disk diffusion assay was conducted in order to investigate the cell protective effect of rAbGSR upon the oxidative stress generated by H₂O₂. The pMAL C5X/AbGSR clone and pMAL-C5X vector transformed ER2523 cells were grown in LB medium containing ampicillin (100 ug/mL) and induced the protein expression for 12 h at 20 °C after 0.5 mM IPTG induction. Subsequently, pMAL C5X/AbGSR was uniformly plated one LB/ampicillin agar plate and pMAL-C5X was placed on another LB/ampicillin agar plate. Three Whatman filter-paper disks (3-mm diameter)

were placed on each agar plate immediately after the inoculation of cultures. Three different volumes (6, 3 and 1.5 μL) of H_2O_2 (11.5 M) were added on each disk of two plates. Plates were incubated overnight at 37 $^\circ\text{C}$ and ranges of clearance were obtained by measuring horizontal and vertical diameters. The graph between H_2O_2 volume and average diameter of range of clearance graph was plotted.

2.5.2. Cell culture and cell viability assays

The Vero cells (African Green Monkey Kidney Epithelial Cells) were cultured in Dulbecco Modified Eagle (DMEM- WELGENE-Korea) culture medium supplemented with 10% fetal bovine serum (FBS), 100 U/mL of penicillin and 100 mg/mL of streptomycin, and the cell line was maintained in 5% CO_2 humidified incubator at 37 $^\circ\text{C}$.

2.5.2.1. MTT assay

A total volume of 100 μL reaction mixture (RM) was prepared by mixing the reagent components as follows: 42 μL of reaction buffer (pH = 7.0), 2 μL of NADPH, 6 μL of GSSG, and 50 μL of rAbGSR (5 ng/ μL). Negative control (NC) was prepared by mixing 92 μL of reaction buffer (pH = 7.0) with 2 μL of NADPH and 6 μL of GSSG. The 2 reactions were incubated for 1 h at room temperature (25 $^\circ\text{C}$) in order to ensure the completion of GSSG to GSH converting reaction.

Pre-cultured Vero cells after reaching the confluence of ~ 80% were seeded in 24 well plates, at the cell density of 1×10^5 cells/mL. The cells in each well were simultaneously treated with the RM and NC. Subsequently cells were treated with 500 μmol of H_2O_2 (0.5 mM) and incubated for 1 h. One group of cell containing wells was remained untreated either with RM, NC or H_2O_2 . Another cell group was treated only with H_2O_2 . Subsequently, cells were incubated with a solution

of 0.5 mg/ml 3-(4, 5-dimethylthiazol-2-yl)-2, 5-diphenyl tetrazolium bromide (MTT) reagent for 30 min at 37⁰C in 5% CO₂ incubator. Then, supernatant was removed and formazan formation was detected by measuring the absorbance at 540 nm using the micro plate reader (Thermo Electron Corporation, Marietta, OH).

2.5.2.2. Flow cytometry

The level of cell protectiveness provided by rAbGSR against H₂O₂ was measured using flow cytometry. The previously mentioned (for MTT assay) RM and NC samples were used for the treatments. The cells were cultured and seeded into a 6 well plate. Cells in one well were treated with RM. Another well was treated with NC. One well from the remaining was treated only with H₂O₂ while another remaining well was kept untreated to detect maximum cell viability. After 24 h of incubation from the treatments, cells in the each well were analyzed by FACSCalibur™ flow cytometer (Becton Dickenson; San Jose, CA), staining with annexin-V FITC (R&D Systems, Minneapolis, MN).

2.6. Investigation of immune related mRNA expression pattern of *AbGSR*

2.6.1. Animal rearing

The healthy disk abalones that were purchased from the Youngsoo commercial abalone farm in Jeju Island, Republic of Korea were screened for 50 g of weight and suitability to the experimental conditions. Predesigned tank system for shellfish rearing at the Marine and Environmental Research Institute of Jeju National University was used for the experiment. Parameters of the tanks were as 250 L capacity and flat bottom, aeration of sand-filtered seawater at a salinity of 34 ± 0.6%

and a temperature of 20 ± 1 °C. Each tank was added with 30 abalones. Animals were pre-acclimatized one week before the experiment under experimental conditions by feeding with fresh marine seaweed (*Undaria pinnatifida*).

2.6.2. Immune challenge experiment, RNA extraction and cDNA synthesis

In order to proceed with the immune challenge experiment, abalones were divided into four separate tanks. Three abalone groups were simultaneously injected with *vibrio parahaemolyticus*, *Listeria monocytogenes* and LPS respectively. One group was treated as an unchallenged control group to collect the data to analyze the tissue specific mRNA expression profile of *AbGSR*. Four healthy unchallenged abalones were dissected to isolate the different tissue types including digestive tract, gill, male gonad, female gonad, mantle and muscle. Hemocytes were isolated by collecting hemolymph from pericardial cavities of abalones and by centrifuging immediately under $3000 \times g$ for 10 min at 4 °C.

In order to conduct the challenge experiment, immune injections were prepared as follows; 100 μ L of 1×10^4 CFU mL^{-1} live bacteria in saline and 100 μ L of LPS ($5 \mu\text{g } \mu\text{L}^{-1}$, *E. coli* 055:B5; Sigma) in saline as an immune stimulant. Each group of abalones was intramuscularly injected with corresponding injection types. At the time points of 3, 6, 12, 24 and 48 h of post challenge, four animals were randomly sampled from each injected abalone groups, and animals were subjected to isolate the hemocytes and gill tissues. Immediate after the isolation, cells and tissues were frozen in liquid nitrogen and subsequently stored in - 80 °C freezer for RNA extraction and cDNA preparation. Total RNA extraction was carried out using TRIzol[®] reagent (Sigma) by following the manufacturer's protocol. Extracted RNA were diluted and pooled to synthesize cDNA using PrimeScript[™] first-strand cDNA synthesis kit (TaKaRa Bio Inc.) according to the manufacturer's

instructions. The resultant cDNA were diluted 40 fold (800 μ L of total volume) and stored at -20°C until further usage for qPCR analysis.

2.6.3. Quantitative real time PCR (qPCR) analysis of mRNA expression levels.

The cDNA prepared upon the RNA extracted from the tissues of normal and immune challenged animals were further used for the quantitative real time PCR (qPCR) and quantitatively analyzed the relative mRNA expression levels of *AbGSR*. The qPCR reactions were conducted by The DiceTM TP800 Real-Time Thermal Cycler System (TaKaRa-Japan). A solution of 4 μ L of diluted cDNA, 7.5 μ L of 2 \times TaKaRa ExTaqTM SYBR premix, 0.6 μ L of sequence specific primers (**Table 1**), and 2.3 μ L of nuclease free distilled H₂O were mixed in the total volume of reaction mixture. The thermal cycling reaction conditions were adjusted as follows: an initial denaturation of 10 sec at 95 $^{\circ}\text{C}$, followed by 40 cycles of 5 sec at 95 $^{\circ}\text{C}$, 10 sec at 58 $^{\circ}\text{C}$ and 20 sec at 72 $^{\circ}\text{C}$, and a final cycle of 15 sec at 95 $^{\circ}\text{C}$, 30 sec at 60 $^{\circ}\text{C}$ and 15 sec at 95 $^{\circ}\text{C}$. The DiceTM Real-Time System Software (version 2.0) automatically set the baseline. The mRNA expression of AbGSR was determined by the Livak method (Livak and Schmittgen, 2001). The expression of internal control gene (ribosomal protein L5- GenBank ID: EF103443) was detected by applying the same qPCR conditions as above. Each qPCR reaction was conducted in triplicates. The 0 h time point (un-injected control) was taken as the baseline. The relative mRNA expression levels were normalized with 0 h time point and expression levels were further normalized to the corresponding saline-injected controls at each time point.

2.7. Statistical analysis

The results from all the experiments were mentioned as mean standard deviation (SD) of triplicates. The intergroup differences were determined by the two-tailed un-paired t-test by comparing the means using GraphPad program (<http://www.graphpad.com/quickcalcs/ttest2/>). Differences were considered to be significant at $P < 0.05$.

Table. 4: Oligomers used in this study (AbGSR)

| Name | purpose | Sequence (5' → 3') |
|------------------|--|---|
| AbGSR- qF | qPCR of <i>AbGSR</i> | ATCCCAGGTGCAGAACACGGTATTT |
| AbGSR- qR | qPCR of <i>AbGSR</i> | TTAAGATTGAGGTGTCGGCTCCAAGG |
| AbGSR- F | Amplification of coding region (NdeI) | GAGAGAcataatgATGCCGCCGGTGGTAAAAAC |
| AbGSR- R | Amplification of coding region (EcoRI) | GAGAGAgaaattcCTATCTCATGGTGACCAGCTCTTCTG |
| abRibI-F | qPCR for abalone RibI | TCACCAACAAGGACATCATTTGTC |
| abRibI-R | qPCR for abalone RibI | CAGGAGGAGTCCAGTGCAGTATG |

3. Results and Discussion

3.1. Sequence identification and Bioinformatics analysis of *AbGSR* cDNA and predicted amino acid sequences

The cDNA sequence of *AbGSR* was identified from our previously established transcriptomic database and it was 2325 bp in length. The lengths of 5'-UTR, ORF and 3'-UTR were 60, 1356 and 909 bp respectively. The amino acid sequence of translated protein (AbGSR) was 452 aa in length. As predicted, molecular weight of AbGSR was 49 kDa with an isoelectric point of 6.6. As per results obtained from the NCBI-CDD and ExPASy-prosite servers, the amino acid sequence possessed a pyridine nucleotide – disulphide oxidoreductase domain (171-246 aa), a Pyridine nucleotide-disulphide oxidoreductase dimerization domain (341-452). Moreover, a Rossmann-fold NAD(P)(+)- binding proteins superfamily signature was also detected in the area of pyridine

nucleotide – disulphide oxidoreductase domain located (171-246 aa) since amino acid sequence corresponding area was consisted of specific structural features that most of the redox enzymes which NAD binding involves such as numerous hydrogen-bonds and van der Waals contacts, in particular H-bonding of residues in a turn between the first strand and the subsequent helix of the Rossmann-fold topology. Entire sequence was further validated as a glutathione reductase family homolog (6-452 aa) since the full amino acid sequence bears important landmarks to be categorized as a glutathione reductase similitude.

3.2. Sequence homology and evolutionary analysis

Table 5 : pairwise sequence alignment (for AbGSR).

| Species | GenBank accession number | Amino acids (aa) | Identity % | Similarity % |
|--------------------------------|---------------------------------|-------------------------|-------------------|---------------------|
| <i>Crassostrea gigas</i> | EKC35400.1 | 452 | 75.7 | 86.7 |
| <i>Loa loa</i> | NP_009016 | 308 | 58.9 | 73.4 |
| <i>Salmo salar</i> | NP_001017950 | 307 | 55.6 | 69.1 |
| <i>Danio rerio</i> | NP_001125838 | 307 | 52.7 | 66.3 |
| <i>Homo sapiens</i> | NP_032073 | 306 | 55.8 | 70.4 |
| <i>Mus musculus</i> | NP_989969 | 315 | 59.1 | 72.9 |
| <i>Columba livia</i> | EMC84573 | 316 | 51.1 | 66.7 |
| <i>Manacus vitellinus</i> | CAJ82730.1 | 299 | 55.6 | 73.0 |
| <i>Drosophila melanogaster</i> | NP_001089049 | 300 | 34.9 | 50.6 |

As per results obtained from pairwise amino acid level sequence comparison, AbGSR showed a sequence similarity of 86.7% and identity of 75.7% with *Crassostrea gigas* as the highest similarity and identity exhibiting its evolutionary relationship with molluscans (**Table 5**). In the constructed multiple sequence alignment, high amino acid conservations were clearly identified over compared species where FAD binding site, glutathione binding site, NADPH binding motif and assembly domain located (**Fig. 10**), which in turn provides the clues on the evolutionary conservation of biochemically important domains.

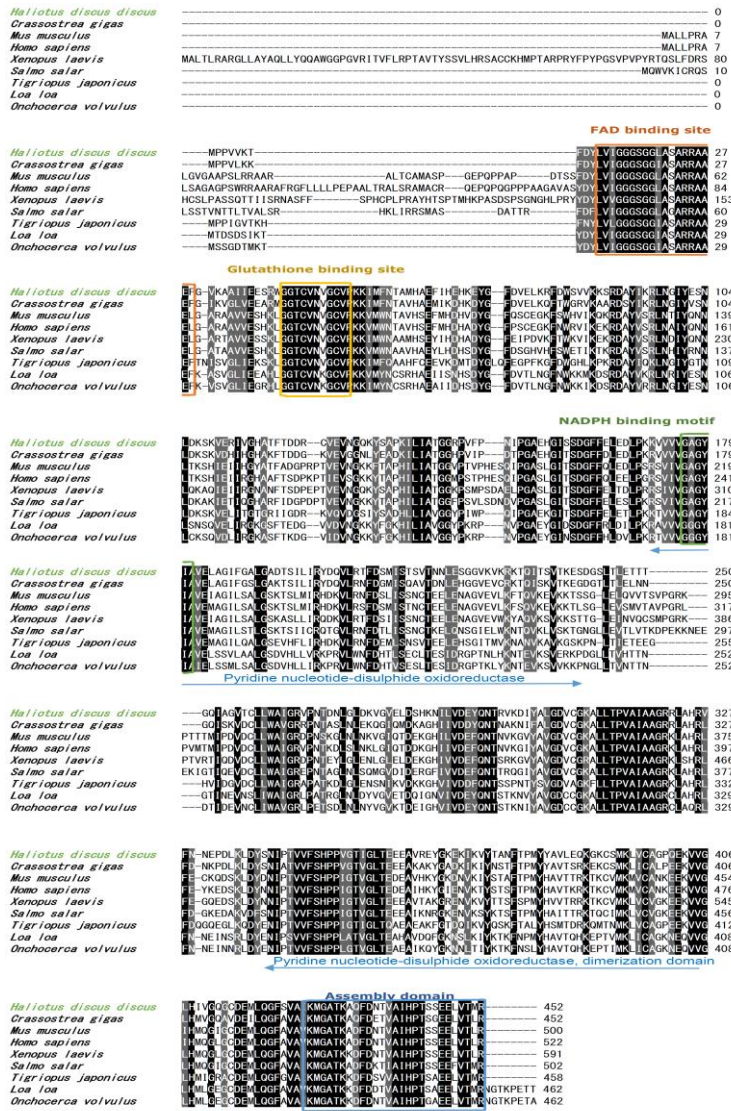
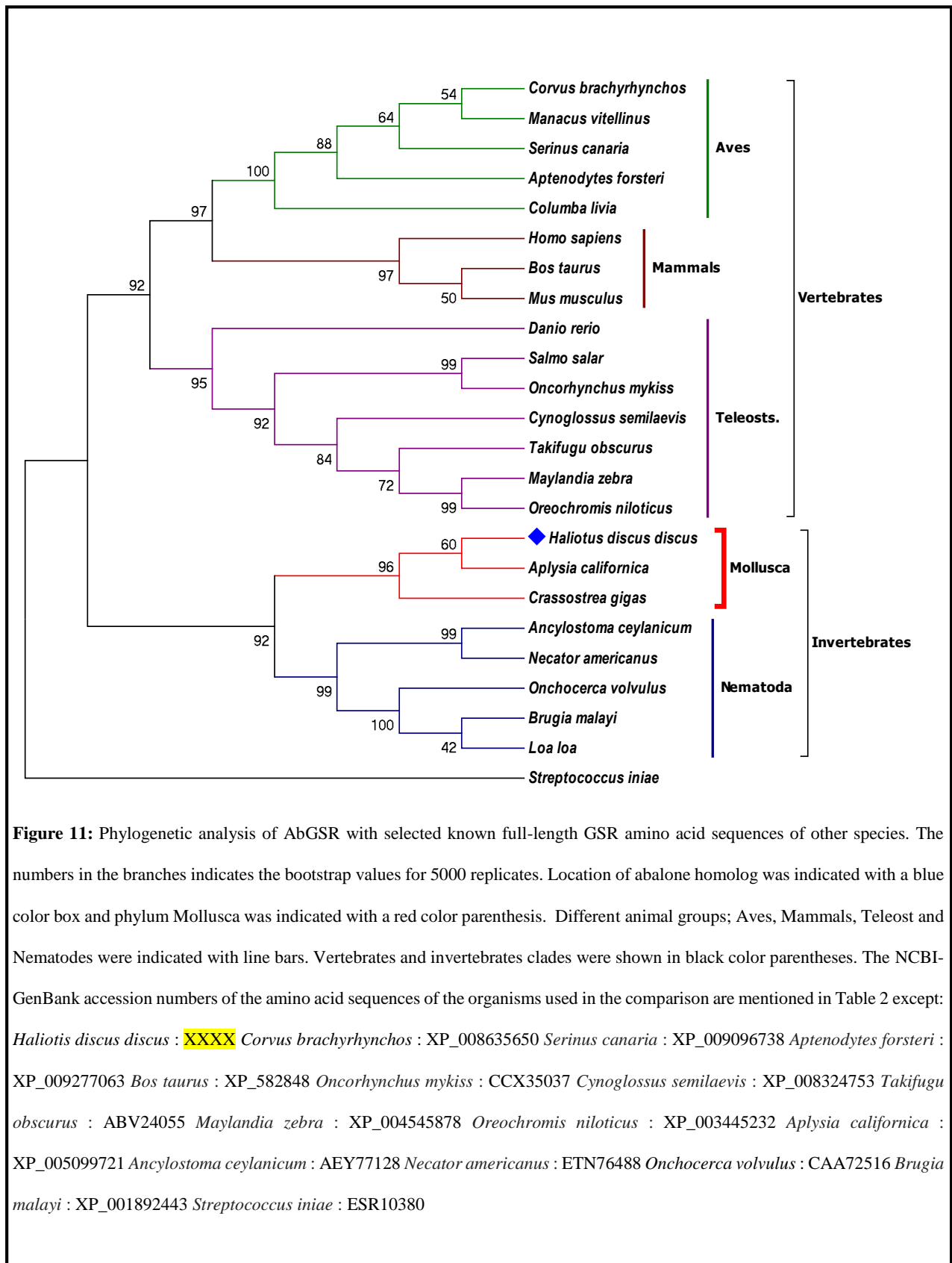


Figure 10: ClustalW multiple sequence alignment of the deduced amino acid sequences of AbGSR with known GSR proteins. The functionally important motifs; FAD binding site, Glutathione binding site, NADPH binding motif assembly domain were indicated with orange color, yellow color, green color and blue color boxes respectively. The pyrimidine nucleotide-disulphide oxidoreductase domain and pyrimidine nucleotide-disulphide oxidoreductase, dimerization domain were indicated with light blue color double headed arrows.

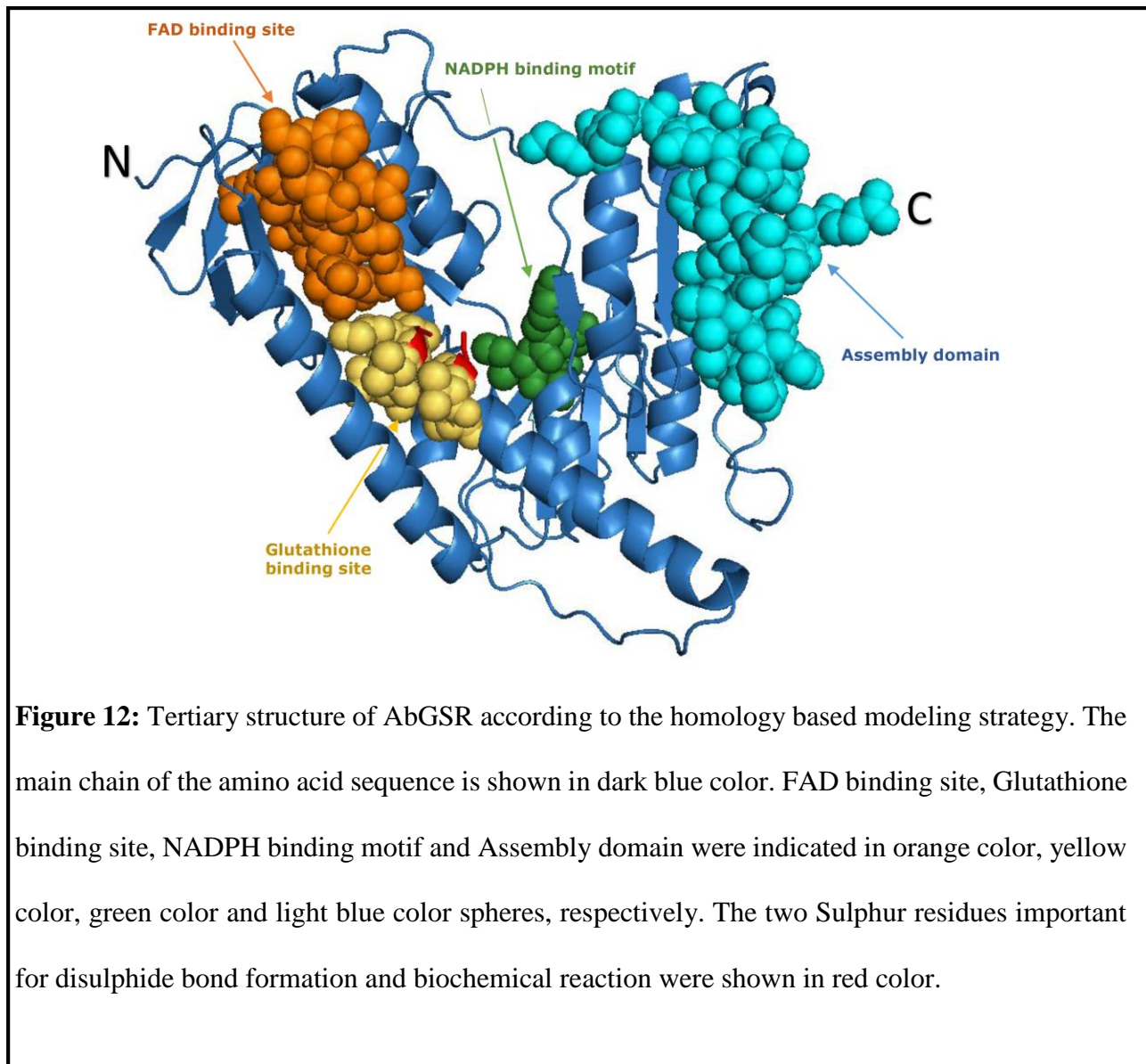
In order to further depict the evolutionary relationship of AbGSR to different GSR sequences identified from other organisms, phylogenetic tree was constructed (**Fig. 11**). According to the information revealed from the phylogenetic tree, AbGSR exhibited the closest evolutionary relationship with *Aplysia californica* and *Crassosrea gigas* by confirming its closest evolutionary relationship with mollscan GSR counterparts. Nematode and molluscan counterparts exhibited two different clades within invertebrates in order to show that they are originated from different ancestors. Examined vertebrate counterparts were separately clustered while showing evolutionarily distance relationships with invertebrates.



3.3. The functional interpretation of AbGSR based on 3D structural features

To visualize the orientations and locations of biochemically important functional motifs and residues in three dimensional manner, 3D structure of AbGSR was generated by applying a homology-based modeling using the online SWISS-MODEL server. As the template, crystal structure of human glutathione reductase resolved to 1.8 Å which shared 64.69% of sequence identity with putative AbGSR amino acid sequence was used (Berkholz et al., 2008). The structural QMEAN4 value for model quality was -0.59.

As observed in the tertiary structure (**Fig. 12**), FAD binding domain, Glutathione binding site and NADPH binding motif were identified to be located closely and one after the other, in order to ensure the efficiency of catalytic reaction. The assembly domain was located in the N- terminal corner of monomeric structure. Moreover, two important sulfur residues responsible for disulfide bond formation and important for the redox reaction identified to be located in glutathione binding site as closely located residues.



3.4. Overexpression and functional properties confirmation of recombinant AbGSR protein

To execute the functional studies on AbGSR, the recombinant AbGSR (rAbGSR), protein was overexpressed in *E.coli* and purified by maltose affinity chromatography. The rAbGSR was run on SDS-PAGE and confirmed the accuracy and purity of obtained protein by observing a single band at the position of 91.5 kDa, confirming the theoretically predicted molecular weight of rAbGSR (49 kDa) as the size of MBP is around 42.5 kDa (**Fig. 13**). As per previous reports, the

monomeric size of recombinantly expressed *Tigriopus* GSR was 55kDa in size which approximately similar to the weight of rAbGSR (Seo et al., 2006). Moreover approximately similar sizes of GSR protein have been previously isolated from tissue and cell extraction of some other organisms (Kubo et al., 1993; Loprasert et al., 2005; Minami et al., 2003; Muller et al., 1997).

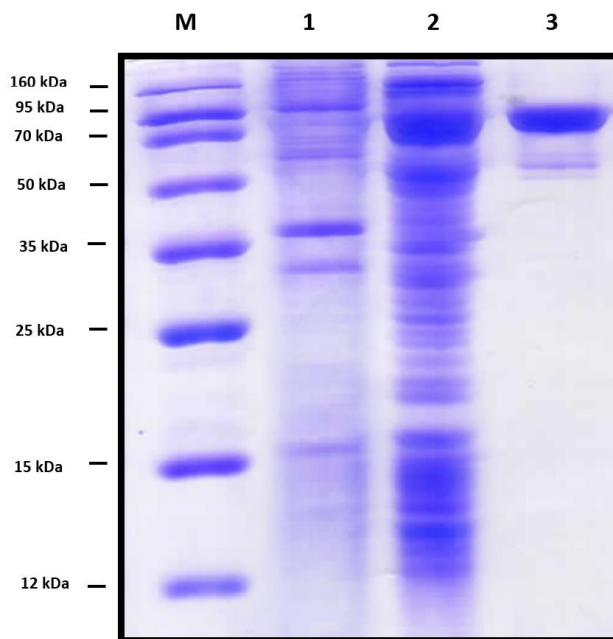


Figure 13: SDS-PAGE analysis of rAbGSR protein. Columns represent: protein marker (M), total cellular extract before IPTG induction (1), recombinant protein in supernatant (crude protein) (2), and eluted AbGSR-MBP protein after purification (3).

As a preliminary step to investigate the biochemical activity of recombinantly expressed AbGSR protein, the activity was tested by adopting a standard GSR activity assay. The assay was conducted following the manufactures instructions and GSR activity (mU/mL) was measured in a gradient of concentrations as dose dependent manner. After plotting the GSR activity (mU/mL) upon different concentrations, a linear graph was observed confirming proper functionality of

rAbGSR (**Fig. 14**). The specific activity obtained from the graph of rAbGSR was 39.5 U/mg. Same activity assay was conducted with MBP protein as the control and no significant activity was detected. Since no significant activity was observed with MBP against GSR specific activity assay, further functional studies were proceeded only with recombinant AbGSR omitting the experiments with MBP protein. As per previous reports, specific activity of recombinant GSR has been reported as 124 U/mg (Seo et al., 2006) from *Tigriopus japonicas*. The purified GSR from human erythrocytes has exhibited a specific activity of 235 U/mg (Krohne-Ehrich et al., 1977).

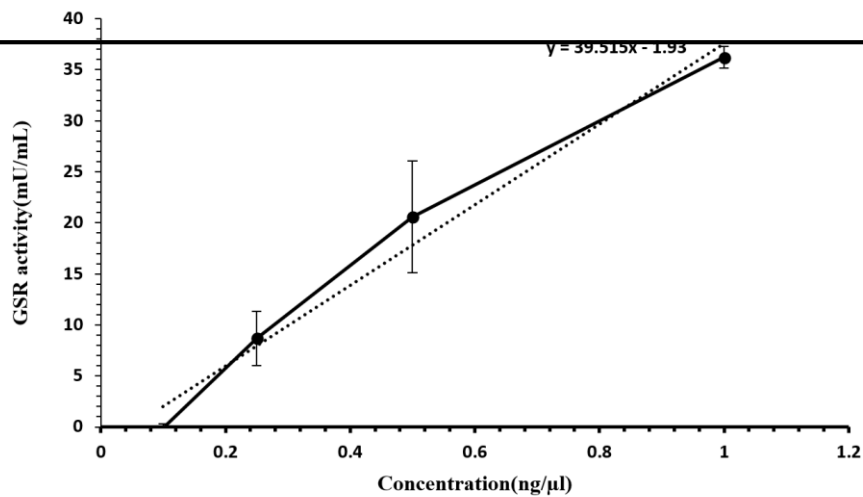


Figure 14: Standard glutathione reductase activity assay using Biovision glutathione reductase activity colorimetric assay kit. The x -axis indicates the protein concentrations; the y -axis indicates the GSR activity.

3.5. Enzymatic properties validation and effect of heavy metals on rAbGSR activity

To further validate the enzymatic properties of rAbGSR, above described assay was conducted against different pH values, different temperature levels, and in the mediums with different ionic strengths.

The assay was conducted in different pH values ranging from 3.0 – 9.0 and optimum pH for the enzymatic reaction was detected at pH 7.0 (**Fig.15A**). The similar optimum pH level has previously been detected with GSR from filarial worm of *setaria cervi* (Arora et al., 2013), rat liver GSR (Mize and Langdon, 1962) and GSR from chicken liver (Erat et al., 2005). As per previous reports, bovine GSR has shown the optimum pH at 7.3 (Erat et al., 2003), while some other lower vertebrates' teleost rainbow trout (Tekman et al., 2008) and diatoms (Arias et al., 2010) have exhibited optimum pH at 8.0. Moreover, assays were conducted under different temperatures ranging from 5.0 – 70.0 °C and optimum temperature for the reaction was detected at 50 °C (**Fig.15B**). Similar optimum temperature level was observed with glutathione reductase purified from chicken liver (Erat et al., 2005) while rainbow trout has exhibited its optimum temperature at lower temperatures such as 10 °C (Tekman et al., 2008). Further, reaction was subjected to the mediums with different ionic strengths ranging from 0-1000 mM. But, no significant effect of changing the medium ionic strength on the rate of enzymatic reaction was observed (**Fig. 15C**).

Heavy metals known to contain different level of toxicological effect on biological organisms ranging from DNA damage to biomolecule degradation (Flora et al., 2008). Inhibitory effect of metals iron such as cadmium upon biochemically important enzymes such carbonic anhydrase from estuarine crab has been extensively studied (Vitale et al., 1999).

Under this circumstance, even though the enzymatic function is known to be inhibited by the effect of heavy metals on various biologically important enzymes, the effect of heavy metals on

molluscan GSR has not been reported yet. Therefore, GSR activity reaction was conducted with rAbGSR in the presence of heavy metal ions such as Cu^{+2} and Cd^{+2} in the medium. The level of inhibitory effect on AbGSR was measured by calculating IC_{50} values. The IC_{50} values obtained for Cu^{+2} and Cd^{+2} were 6 and 0.75 mM respectively (**Fig. 15D I. and II.**). With respect to GSR, inhibitory effect of ranges of metal ions have been investigated with GSR from human erythrocytes (Coban et al., 2007), and with teleost such as rainbow trout GSR (Tekman et al., 2008). In each case, as observed with current study, activity of GSRs have been greatly affected by the metal ions in the medium.

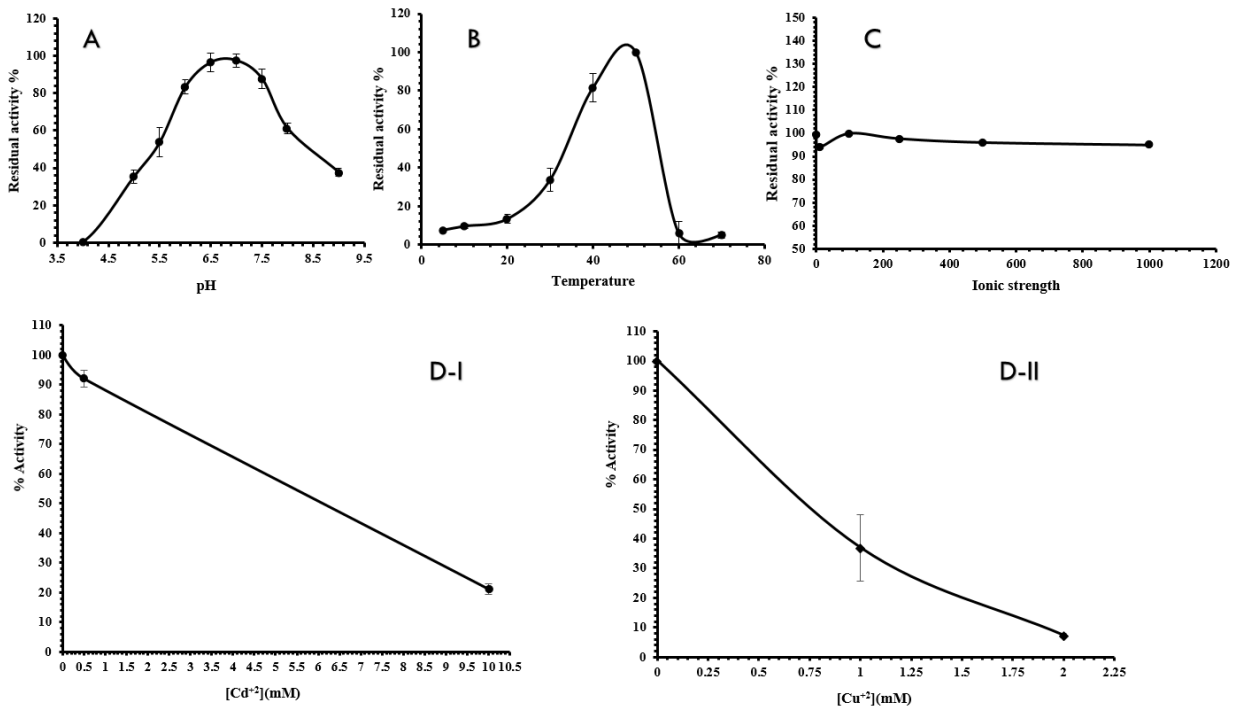


Figure 15: The enzymatic properties of rAbGSR protein. (A) The optimum pH graph. The *x*-axis indicates the pH value in the medium; (B) The optimum temperature graph. The *x*-axis indicates the protein concentrations; (C) The optimum pH graph. The *x*-axis indicates the protein concentrations; in each graph the *y*-axis indicates the average absorbance at 405 nm (D) Inhibitory effect of heavy metal ions. 1. Effect of Cd²⁺. The *x*-axis indicates the protein concentrations; 2. Effect of Cu²⁺. The *x*-axis indicates the protein concentrations; in both graphs the *y*-axis indicates % activity. Error bars represent the SD (n = 3).

3.6. Involvement of AbGSR in antioxidant defense mechanisms

Glutathione reductase is the key enzymatic counterpart, which catalyzes the conversion of glutathione oxidized form (GSSG) into reduced form (GSH). Since presence of proper GSH concentration levels and proper ratio of GSH/GSSG is important for further execution of H₂O₂ oxidative reaction, GSR holds a major involvement as an antioxidant by catalyzing the above mentioned reaction. Even though, this phenomenon is well studied and involvement of GSR is known to be significant in antioxidant defense (Deponete, 2013), none of the studies have undergone in order to detect the significance of molluscan GSR counterparts as antioxidants. Therefore, in current study we put our effort forward to identify and present the antioxidant involvement of AbGSR.

In order to obtain a preliminary insight on AbGSR antioxidant effect, we initially conducted a disk diffusion antioxidant assay which has previously been performed to study the antioxidant properties of antioxidants species such as Glutathione S-transferases (GSTs) (Lee et al., 2007) and peroxiredoxins (Park et al., 2005). The range of clearance from AbGSR overexpressed plates in the presence of H₂O₂ was significantly lower ($p < 0.05$) compared to MBP overexpressed plates (**Fig. 16A and Fig. 17**). Since a considerable cell protective effect has been detected with preliminary antioxidant assay conducted by overexpressing AbGSR in *E. coli*, studies were further extended to analyze antioxidant properties mediated by AbGSR. As previously observed with other antioxidant species, with the overexpression of AbGSR in *E. coli*, confirming the importance of maintaining GSH/GSSG ratio for antioxidant defense, our preliminary experiment exhibited a detectable cell protective effect against H₂O₂. The insights on GSR activity has been previously

obtained with the vector borne GSR complementation studies conducted with GR-deficient mutant strain of *E. coli* (SG5) (Kunert et al., 1990).

To depict the picture on significance of cell protectiveness provided by rAbGSR, MTT assay was conducted. The negative control (NC) was used in order to check whether any cell protectiveness effect is generated due to the reaction buffer and substrates used. A cell sample was remained untreated by assuming the 100 % viability of cells in order to compare the viable cell levels in treatments. Another cell sample was treated only with H₂O₂ to identify the maximum level of cell death effect caused by H₂O₂. As per result observed in MTT assay, Cells treated only with H₂O₂ exhibited approx. 47% of cell survival compared to untreated control sample. Cells treated with NC showed approx. 49% of cell survival. Interestingly, cell sample which was incubated with the RM exhibited significantly increased cell survival effect ($p < 0.05$) compared to the cells treated only with H₂O₂ even though NC did not exhibit significant cell protective effect compared to H₂O₂ treated sample. Therefore, rAbGSR has shown a considerable cell protective effect against the oxidative stress generated by exogenous H₂O₂ (**Fig. 16B**).

Evidences were gathered by subjecting the samples with flow cytometric analysis methods, to further prove the cell protective effect against H₂O₂ mediated by glutathione generating enzymatic reaction which is catalyzed by AbGSR. All the samples (RM, NC, untreated cells and only H₂O₂ treated cells) subjected to analyze with flow cytometry after staining with annexin-V. As per obtained graphs, control cells remained untreated with H₂O₂ exhibited a low level annexin-V staining (1.77 %) conforming the higher number of cell survival in the sample. Neighboring two samples, one treated with only with H₂O₂ and other with NC and then with H₂O₂ exhibited highest cell death rates over annexin-V staining (51.5 and 48.4 % respectively). The cell sample treated with RM and then with H₂O₂ has exhibited a 20.6 % annexin-V staining value confirming

retroverted force on the cell death effect developed on Vero cells due to addition of H₂O₂ in the medium (**Fig. 16C**). Above observation were also reinforced by our microscopic observation of the cells used in each experiment (**Fig. 18**).

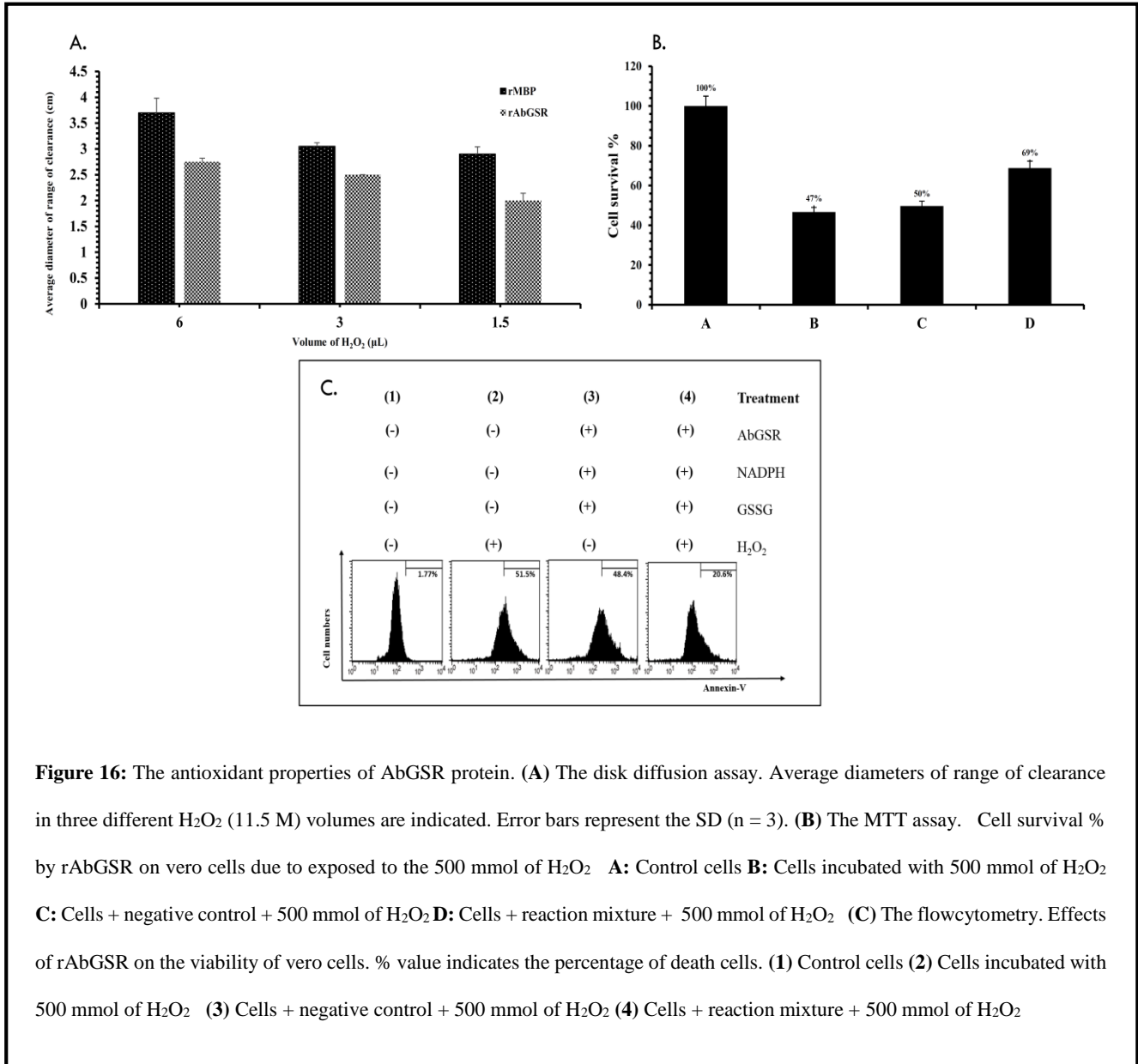


Figure 16: The antioxidant properties of AbGSR protein. **(A)** The disk diffusion assay. Average diameters of range of clearance in three different H₂O₂ (11.5 M) volumes are indicated. Error bars represent the SD (n = 3). **(B)** The MTT assay. Cell survival % by rAbGSR on vero cells due to exposed to the 500 mmol of H₂O₂ **A:** Control cells **B:** Cells incubated with 500 mmol of H₂O₂ **C:** Cells + negative control + 500 mmol of H₂O₂ **D:** Cells + reaction mixture + 500 mmol of H₂O₂ **(C)** The flowcytometry. Effects of rAbGSR on the viability of vero cells. % value indicates the percentage of death cells. **(1)** Control cells **(2)** Cells incubated with 500 mmol of H₂O₂ **(3)** Cells + negative control + 500 mmol of H₂O₂ **(4)** Cells + reaction mixture + 500 mmol of H₂O₂

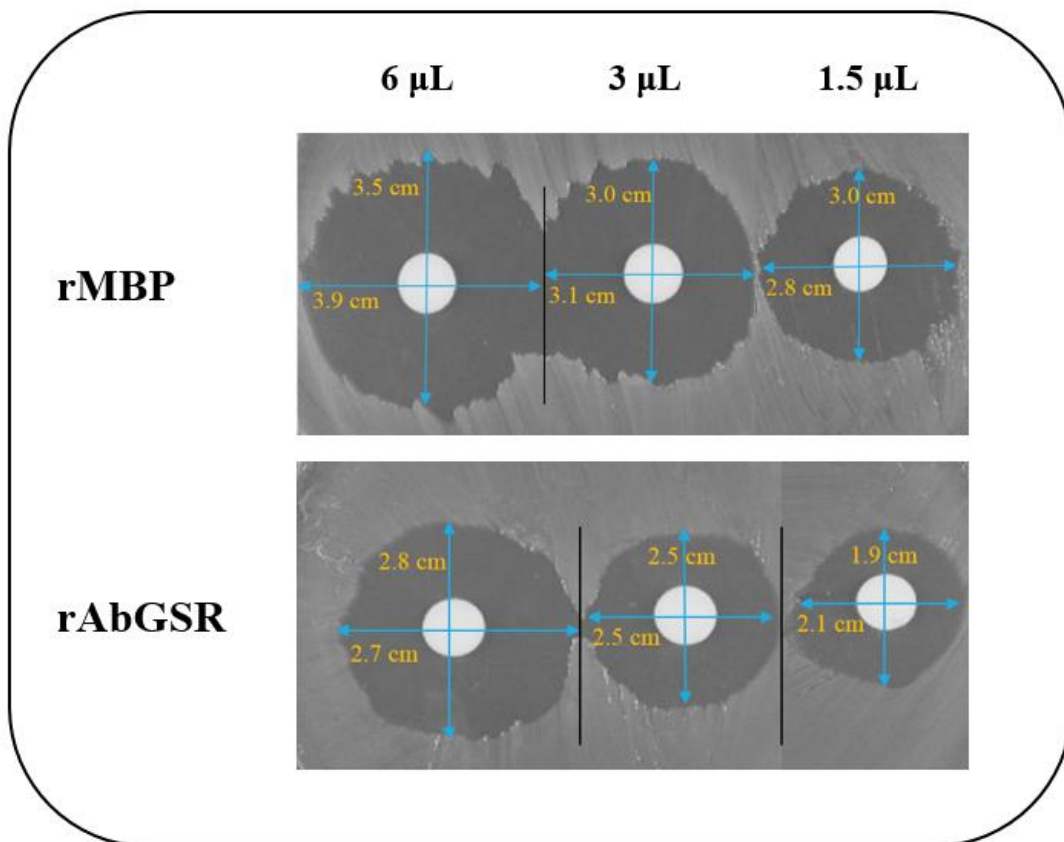
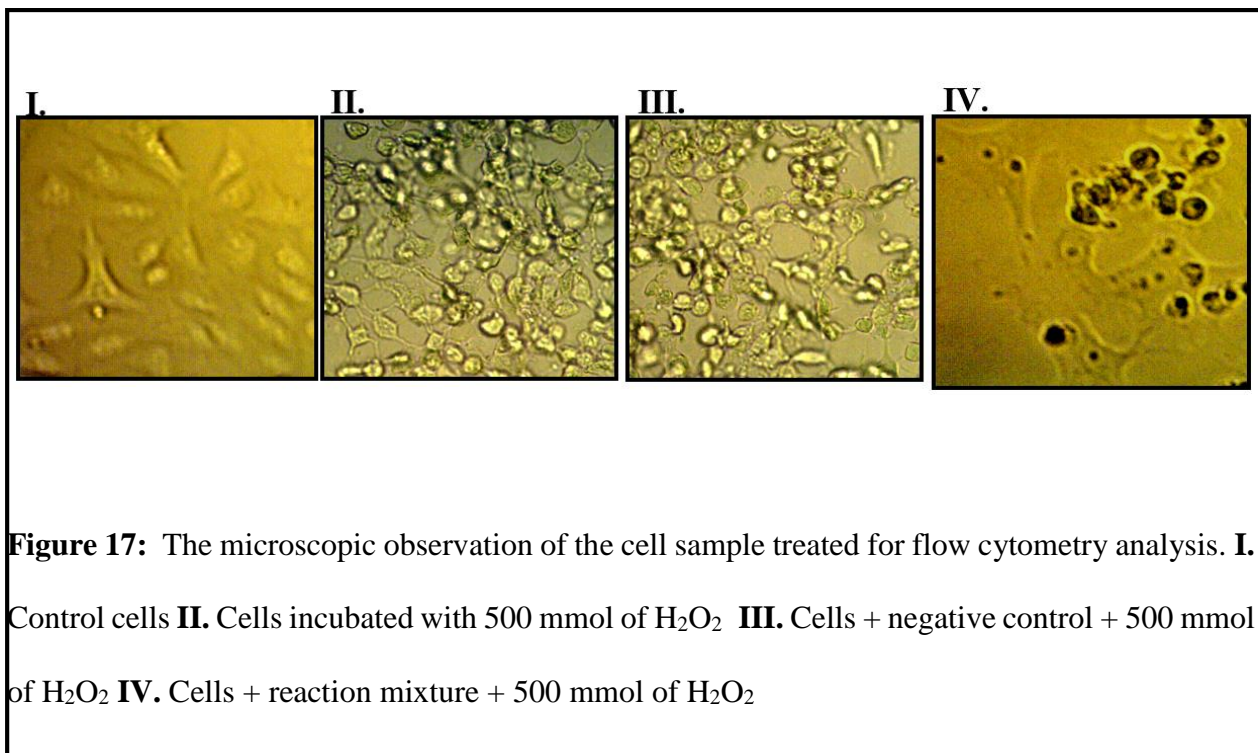


Figure 16: rMBP and rAbGSR overexpressed in ER2523 cells and plated on LB/Amp agar plates. H₂O₂ was blotted on Whatman filter papers as a gradient of volumes (6, 3 and 1.5 μL) and ranges of clearance were measured on following day. Blue color double headed arrows indicate the vertical and horizontal diameters.

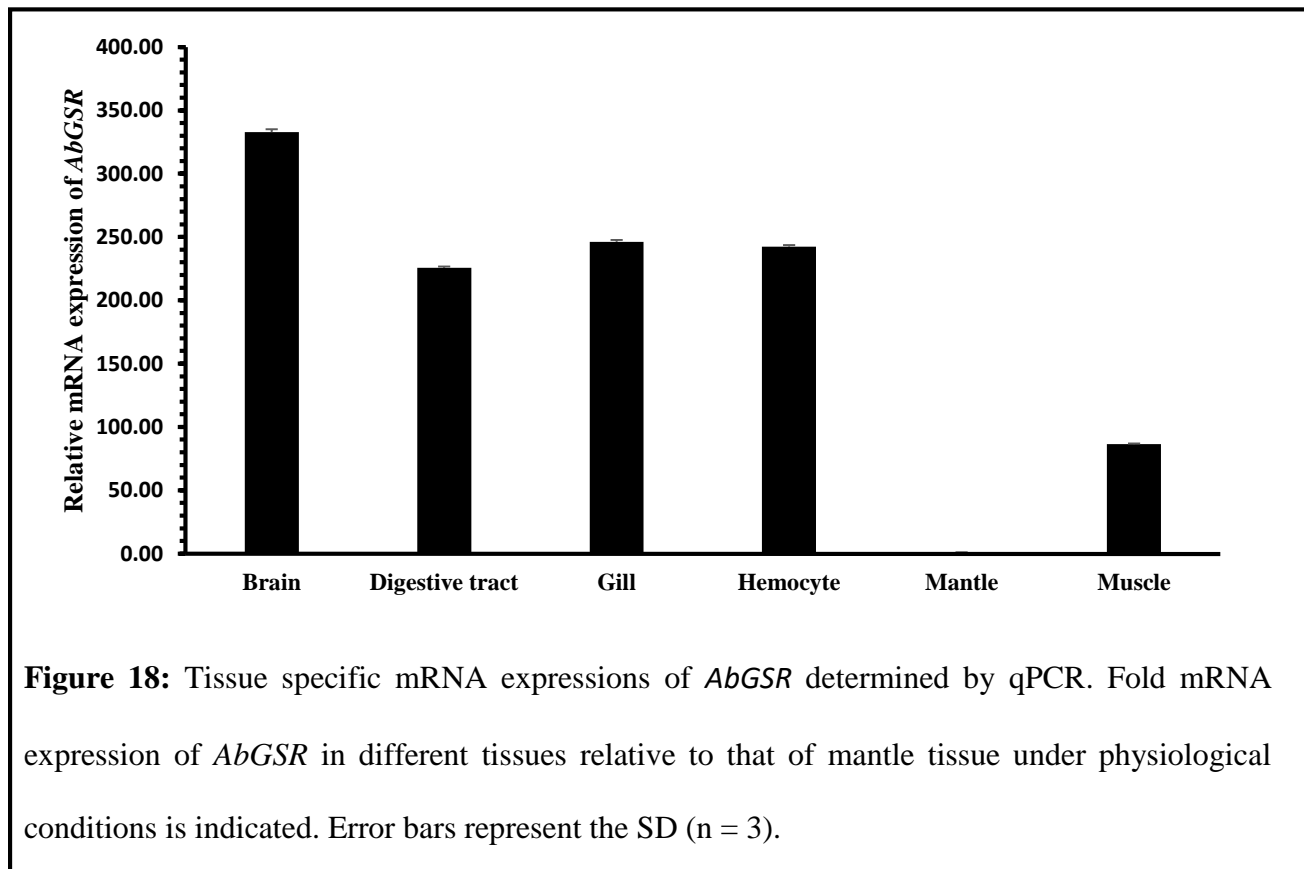


Specific approaches in order to detect antioxidant importance of GSR in previous studies conducted with mammalian have put forward. Some studies have shown that the inhibition of GSR by 1,3-bis (2-chloroethyl)-1-nitrosourea (BCNU) in tumor cells exhibits the less capability to resist the respiratory burst of activated macrophages (Reed, 1985) while a different study conducted with BCNU-treated liver cells has shown that they were highly susceptible to adriamycin-mediated oxidative stress (Dolphin et al., 1989). Moreover, when GSR gene was suppressed by antisense gene transfection in hamster CHO cells, cells have exhibited higher susceptible for oxidant injuries (Hansen et al., 1993)

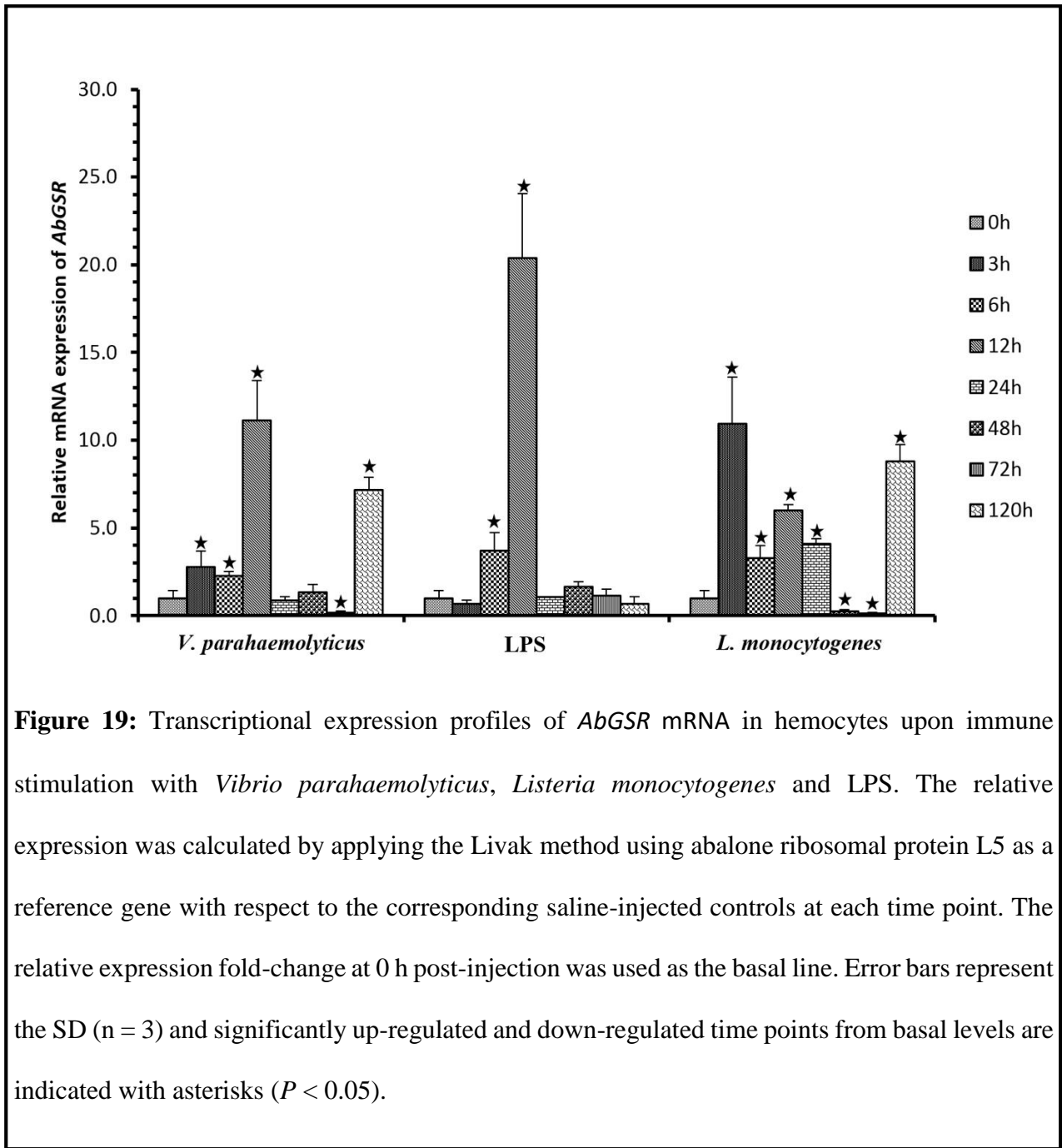
Particularly in the current study conducted with rAbGSR molecule, we have assembled the first insight into the antioxidant properties of a GSR homolog from molluscan species using different approaches to assess AbGSR antioxidant defensive properties while breaking the estimation on significance of cell protective level provided by AbGSR.

3.7. qPCR analysis of *AbGSR* tissue specific mRNA expression and immune related expression patterns

To investigate the *AbGSR* mRNA expressional behavior at tissue specific manner, *AbGSR* transcripts were quantified using qPCR methods. Six distinguishable tissues (brain, digestive tract, gill, hemocytes, muscle and mantle) from abalones were detached and subjected to mRNA quantification. In resultant profile, the mRNA expression was observed to be ubiquitous in all tissues examined except mantle. Next to the mantle, least expressional levels were detected in muscle tissue while brain shows the highest expressions. Gill, hemocytes and digestive tract exhibited moderate expressional levels. In overall, the obtained results reflects the diverse role of *AbGSR* in tissue specific manner (**Fig. 18**).



The comprehensive studies have been undergone with mammalian models such as mice, in order to demonstrate the essence of GSR counterparts in host defense against deferent type of model bacterial organisms (Yan et al., 2012; Yan et al., 2013). Despite the presence of such studies with mammals, none of the studies have undergone to detect the involvement of GSR counterparts in sepsis condition with respect to molluscan biota. In this regards, we drove our studies into a direction to detect whether *AbGSR* gene is expressed under immunologically challenged conditions. To identify whether *AbGSR* has any immune related behavior in the level of gene expression, *AbGSR* mRNA expression was examined upon the infection of *V. parahaemolyticus* and *L. monocytogenes*, and administration of LPS. After challenge with pathogenic agents, hemocytes from animals were subjected for mRNA expressional analysis. Upon the infectious conditions, expressional levels of *AbGSR* were significantly elevated with *V. parahaemolyticus* at 3 h, 6 h, 12 h and 120 h while showing highest expressional levels at 12 h. With LPS, both 6 h and 12 h time points were significantly induced while having highest expressional levels at 12 h. with respect to *L. monocytogenes*, mRNA expressional levels were significantly induced at the time point of 3 h, 6 h, 12 h, 24 h and 120 h time points while showing the highest expressional levels at 3h (**Fig. 19**). According to the obtained results, since potent inductions of mRNA expressional levels have been detected with *AbGSR* under immunologically challenged conditions, we can also suspect the involvement of *AbGSR* in host defense by facilitating the mechanisms such as important to the development of neutrophil extracellular traps, and by sustaining phagocytic oxidative bursts as already identified with mammalian models (Yan et al., 2012). Further studies need to be conducted in this regards, in order to identify the factual involvement of *AbGSR* in abalone immunity.



3.8. Conclusion.

In conclusion, we have identified a glutathione reductase homolog (AbGSR) from disk abalone. Its molecular properties were analyzed and predictions on structural and functional properties were made using bioinformatics tools. The putative *AbGSR* cDNA sequence bears important functional motifs corresponding for catalytic activity. Further, recombinant protein was overexpressed in order to analyze its primary biochemical properties and secondary level antioxidant properties. rAbGSR exhibited positive results against the standard GSR assay while giving optimum levels for general enzymatic properties. Moreover, rAbGSR showed a detectable cell protective effect against disk diffusion assay and significant levels of cell protectiveness against MTT assay and flow cytometry. Ultimately, mRNA expressional levels were quantified in tissue specific manner and immune stimulated conditions, to obtain the insight of AbGSR distribution in tissue-wise manner and the behavior of gene expressional levels under pathogenic infectious conditions. The tissue specific mRNA expressional levels were found to be ubiquitous and mRNA expressional levels were modulated upon the pathogenic challenges conducted with *V. parahaemolyticus*, *L. monocytogenes* and LPS. In overall, current study broaden up the existing knowledge on GSR into molluscan biota while showing AbGSR antioxidant properties and providing insight into the immunological importance of AbGSR similitude.

References

1. Abe, Y., Nagata, R., Hasunuma, Y., Yokosawa, H., 2001. Isolation, characterization and cDNA cloning of a one-lobed transferrin from the ascidian *Halocynthia roretzi*. *Comparative biochemistry and physiology. Part B, Biochemistry & molecular biology* 128, 73-79.
2. Aisen, P., 1989. *Physical biochemistry of the transferrins*. VCH Publishers, New York.
3. Aisen, P., 2004. Transferrin receptor 1. *The international journal of biochemistry & cell biology* 36, 2137-2143.
4. Archibald, F., 1983. *Lactobacillus plantarum*, an organism not requiring iron. *FEMS Microbiology Letters* 19, 29–32.
5. Arnold, K., Bordoli, L., Kopp, J., Schwede, T., 2006. The SWISS-MODEL workspace: a web-based environment for protein structure homology modelling. *Bioinformatics* 22, 195-201.
6. Bayne, C.J., Gerwick, L., Fujiki, K., Nakao, M., Yano, T., 2001. Immune-relevant (including acute phase) genes identified in the livers of rainbow trout, *Oncorhynchus mykiss*, by means of suppression subtractive hybridization. *Developmental and comparative immunology* 25, 205-217.
7. Beutler, E., Gelbart, T., Lee, P., Trevino, R., Fernandez, M.A., Fairbanks, V.F., 2000. Molecular characterization of a case of atransferrinemia. *Blood* 96, 4071-4074.
8. Bradford, M.M., 1976. A rapid and sensitive method for the quantitation of microgram quantities of protein utilizing the principle of protein-dye binding. *Analytical biochemistry* 72, 248-254.
9. Brooks, J.M., Wessel, G.M., 2002. The major yolk protein in sea urchins is a transferrin-like, iron binding protein. *Developmental biology* 245, 1-12.
10. Brown, J.P., Hewick, R.M., Hellstrom, I., Hellstrom, K.E., Doolittle, R.F., Dreyer, W.J., 1982. Human melanoma-associated antigen p97 is structurally and functionally related to transferrin. *Nature* 296, 171-173.
11. Bruyneel, B., Woestyne, M.v., Verstraete, W., 1989. Lactic acid bacteria: Micro-organisms able to grow in the absence of available iron and copper. *Biotechnology Letters* 11, 401-406.
12. Casadevall, A., Pirofski, L., 2001. Host-pathogen interactions: the attributes of virulence. *The Journal of infectious diseases* 184, 337-344.
13. Elston, R., Wood, G.S.L., 1983. Pathogenesis of vibriosis in cultured juvenile red abalone, *Haliotis rufescens* Swainson. *Journal of Fish Diseases* 6, 111–128.
14. Fisher, M., Gokhman, I., Pick, U., Zamir, A., 1997. A structurally novel transferrin-like protein accumulates in the plasma membrane of the unicellular green alga *Dunaliella salina* grown in high salinities. *The Journal of biological chemistry* 272, 1565-1570.
15. Fisher, M., Zamir, A., Pick, U., 1998. Iron uptake by the halotolerant alga *Dunaliella* is mediated by a plasma membrane transferrin. *The Journal of biological chemistry* 273, 17553-17558.
16. Gao, J., Ding, S., Huang, X., Shi, X., 2013. Cloning and expression characterization of the serum transferrin gene in the Chinese black sleeper (*Bostrichthys sinensis*). *Gene* 515, 89-98.
17. Goggin, C., Lester, R., 1995. *Perkinsus*, a protistan parasite of abalone in Australia: A review. *Marine and Freshwater Research* 46, 639 - 646.

18. Gomme, P.T., McCann, K.B., Bertolini, J., 2005. Transferrin: structure, function and potential therapeutic actions. *Drug discovery today* 10, 267-273.
19. Guz, N., Attardo, G.M., Wu, Y., Aksoy, S., 2007. Molecular aspects of transferrin expression in the tsetse fly (*Glossina morsitans morsitans*). *Journal of insect physiology* 53, 715-723.
20. Huang, C.Y., Liu, P.C., Lee, K.K., 2001. Withering syndrome of the small abalone, *Haliotis diversicolor supertexta*, is caused by *Vibrio parahaemolyticus* and associated with thermal induction. *Zeitschrift fur Naturforschung. C, Journal of biosciences* 56, 898-901.
21. Jamroz, R.C., Gasdaska, J.R., Bradfield, J.Y., Law, J.H., 1993. Transferrin in a cockroach: molecular cloning, characterization, and suppression by juvenile hormone. *Proceedings of the National Academy of Sciences of the United States of America* 90, 1320-1324.
22. Jurecka, P., Imazarow, I., Stafford, J.L., Ruszczuk, A., Taverne, N., Belosevic, M., Savelkoul, H.F., Wiegertjes, G.F., 2009. The induction of nitric oxide response of carp macrophages by transferrin is influenced by the allelic diversity of the molecule. *Fish & shellfish immunology* 26, 632-638.
23. Kim, B.Y., Lee, K.S., Choo, Y.M., Kim, I., Hwang, J.S., Sohn, H.D., Jin, B.R., 2008. Molecular cloning and characterization of a transferrin cDNA from the white-spotted flower chafer, *Protaetia brevitarsis*. *DNA sequence : the journal of DNA sequencing and mapping* 19, 146-150.
24. Lambert, L.A., Perri, H., Halbrooks, P.J., Mason, A.B., 2005a. Evolution of the transferrin family: conservation of residues associated with iron and anion binding. *Comparative biochemistry and physiology. Part B, Biochemistry & molecular biology* 142, 129-141.
25. Lambert, L.A., Perri, H., Meehan, T.J., 2005b. Evolution of duplications in the transferrin family of proteins. *Comparative biochemistry and physiology. Part B, Biochemistry & molecular biology* 140, 11-25.
26. Lee, K.K., Liu, P.C., Huang, C.Y., 2003. *Vibrio parahaemolyticus* infectious for both humans and edible mollusk abalone. *Microbes and infection / Institut Pasteur* 5, 481-485.
27. Lee, K.S., Kim, B.Y., Kim, H.J., Seo, S.J., Yoon, H.J., Choi, Y.S., Kim, I., Han, Y.S., Je, Y.H., Lee, S.M., Kim, D.H., Sohn, H.D., Jin, B.R., 2006. Transferrin inhibits stress-induced apoptosis in a beetle. *Free radical biology & medicine* 41, 1151-1161.
28. Lee, Y., De Zoysa, M., Whang, I., Lee, S., Kim, Y., Oh, C., Choi, C.Y., Yeo, S.Y., Lee, J., 2011. Molluscan death effector domain (DED)-containing caspase-8 gene from disk abalone (*Haliotis discus discus*): molecular characterization and expression analysis. *Fish & shellfish immunology* 30, 480-487.
29. Lenarcic, B., Krishnan, G., Borukhovich, R., Ruck, B., Turk, V., Moczydowski, E., 2000. Saxiphilin, a saxitoxin-binding protein with two thyroglobulin type 1 domains, is an inhibitor of papain-like cysteine proteinases. *The Journal of biological chemistry* 275, 15572-15577.
30. Liu, J., Zhang, S., Li, L., 2009. A transferrin-like homolog in amphioxus *Branchiostoma belcheri*: Identification, expression and functional characterization. *Molecular immunology* 46, 3117-3124.
31. Liu, P.C., Chen, Y.C., Huang, C.Y., Lee, K.K., 2000. Virulence of *Vibrio parahaemolyticus* isolated from cultured small abalone, *Haliotis diversicolor supertexta*, with withering syndrome. *Letters in applied microbiology* 31, 433-437.
32. Livak, K.J., Schmittgen, T.D., 2001. Analysis of relative gene expression data using real-time quantitative PCR and the 2⁻($\Delta\Delta C(T)$) Method. *Methods* 25, 402-408.

33. Marchler-Bauer, A., Lu, S., Anderson, J.B., Chitsaz, F., Derbyshire, M.K., DeWeese-Scott, C., Fong, J.H., Geer, L.Y., Geer, R.C., Gonzales, N.R., Gwadz, M., Hurwitz, D.I., Jackson, J.D., Ke, Z., Lanczycki, C.J., Lu, F., Marchler, G.H., Mullokandov, M., Omelchenko, M.V., Robertson, C.L., Song, J.S., Thanki, N., Yamashita, R.A., Zhang, D., Zhang, N., Zheng, C., Bryant, S.H., 2011. CDD: a Conserved Domain Database for the functional annotation of proteins. *Nucleic acids research* 39, D225-229.
34. Morabito, M.A., Moczydlowski, E., 1994. Molecular cloning of bullfrog saxiphilin: a unique relative of the transferrin family that binds saxitoxin. *Proceedings of the National Academy of Sciences of the United States of America* 91, 2478-2482.
35. Murayama, E., Okuno, A., Ohira, T., Takagi, Y., Nagasawa, H., 2000. Molecular cloning and expression of an otolith matrix protein cDNA from the rainbow trout, *Oncorhynchus mykiss*. *Comparative biochemistry and physiology. Part B, Biochemistry & molecular biology* 126, 511-520.
36. Nakatsugawa, T., Nagai, T., Hiya, T., Nishizawa, T., Muroga, K., 1999. A virus isolated from juvenile Japanese black abalone *Nordotis discus discus* affected with amyotrophy, *Diseases of aquatic organisms*, pp. 159-161.
37. Nichol, H., Law, J.H., Winzerling, J.J., 2002. Iron metabolism in insects. *Annual review of entomology* 47, 535-559.
38. Noinaj, N., Easley, N.C., Oke, M., Mizuno, N., Gumbart, J., Boura, E., Steere, A.N., Zak, O., Aisen, P., Tajkhorshid, E., Evans, R.W., Goringe, A.R., Mason, A.B., Steven, A.C., Buchanan, S.K., 2012. Structural basis for iron piracy by pathogenic *Neisseria*. *Nature* 483, 53-58.
39. Ong, S.T., Ho, J.Z., Ho, B., Ding, J.L., 2006. Iron-withholding strategy in innate immunity. *Immunobiology* 211, 295-314.
40. Pandey, A., Bringel, F., Meyer, J.-M., 1994. Iron requirement and search for siderophores in lactic acid bacteria. *Applied Microbiology and Biotechnology* 40, 735-739.
41. Patel, S.S., Carr, B.R., 2008. Oocyte quality in adult polycystic ovary syndrome. *Seminars in reproductive medicine* 26, 196-203.
42. Rose, T.M., Plowman, G.D., Teplow, D.B., Dreyer, W.J., Hellstrom, K.E., Brown, J.P., 1986. Primary structure of the human melanoma-associated antigen p97 (melanotransferrin) deduced from the mRNA sequence. *Proceedings of the National Academy of Sciences of the United States of America* 83, 1261-1265.
43. Sahoo, P.K., Mohanty, B.R., Kumari, J., Barat, A., Sarangi, N., 2009. Cloning, nucleotide sequence and phylogenetic analyses, and tissue-specific expression of the transferrin gene in *Cirrhinus mrigala* infected with *Aeromonas hydrophila*. *Comparative immunology, microbiology and infectious diseases* 32, 527-537.
44. Schreiber, G., Dryburgh, H., Millership, A., Matsuda, Y., Inglis, A., Phillips, J., Edwards, K., Maggs, J., 1979. The synthesis and secretion of rat transferrin. *The Journal of biological chemistry* 254, 12013-12019.
45. Schwarz, M., Sal-Man, N., Zamir, A., Pick, U., 2003. A transferrin-like protein that does not bind iron is induced by iron deficiency in the alga *Dunaliella salina*. *Biochimica et biophysica acta* 1649, 190-200.
46. Schwyn, B., Neilands, J.B., 1987. Universal chemical assay for the detection and determination of siderophores. *Analytical biochemistry* 160, 47-56.

47. Stafford, J.L., Belosevic, M., 2003. Transferrin and the innate immune response of fish: identification of a novel mechanism of macrophage activation. *Developmental and comparative immunology* 27, 539-554.
48. Stafford, J.L., Neumann, N.F., Belosevic, M., 2001. Products of proteolytic cleavage of transferrin induce nitric oxide response of goldfish macrophages. *Developmental and comparative immunology* 25, 101-115.
49. Suryo Rahmanto, Y., Bal, S., Loh, K.H., Yu, Y., Richardson, D.R., 2012. Melanotransferrin: search for a function. *Biochimica et biophysica acta* 1820, 237-243.
50. Tamura, K., Stecher, G., Peterson, D., Filipski, A., Kumar, S., 2013. MEGA6: Molecular Evolutionary Genetics Analysis version 6.0 Molecular Biology and Evolution.
51. Thelander, L., Graslund, A., Thelander, M., 1983. Continual presence of oxygen and iron required for mammalian ribonucleotide reduction: possible regulation mechanism. *Biochemical and biophysical research communications* 110, 859-865.
52. Thompson, G.J., Crozier, Y.C., Crozier, R.H., 2003. Isolation and characterization of a termite transferrin gene up-regulated on infection. *Insect molecular biology* 12, 1-7.
53. Thompson, J.D., Higgins, D.G., Gibson, T.J., 1994. CLUSTAL W: improving the sensitivity of progressive multiple sequence alignment through sequence weighting, position-specific gap penalties and weight matrix choice. *Nucleic Acids Res* 22, 4673-4680.
54. Toe, A., Areechon, N., Srisapoome, P., 2012. Molecular characterization and immunological response analysis of a novel transferrin-like, pacifastin heavy chain protein in giant freshwater prawn, *Macrobrachium rosenbergii* (De Man, 1879). *Fish & shellfish immunology* 33, 801-812.
55. Uribe, C., Folch, H., Enriquez, R., Moran, G., 2011. Innate and adaptive immunity in teleost fish: a review. *Veterinari Medicina* 56, 486-503.
56. Wally, J., Halbrooks, P.J., Vonrhein, C., Rould, M.A., Everse, S.J., Mason, A.B., Buchanan, S.K., 2006. The crystal structure of iron-free human serum transferrin provides insight into inter-lobe communication and receptor binding. *The Journal of biological chemistry* 281, 24934-24944.
57. WL, D., PyMOL: An Open-Source Molecular Graphics Tool.
58. Yoshiga, T., Georgieva, T., Dunkov, B.C., Harizanova, N., Ralchev, K., Law, J.H., 1999. *Drosophila melanogaster* transferrin. Cloning, deduced protein sequence, expression during the life cycle, gene localization and up-regulation on bacterial infection. *European journal of biochemistry / FEBS* 260, 414-420.
59. Yoshiga, T., Hernandez, V.P., Fallon, A.M., Law, J.H., 1997. Mosquito transferrin, an acute-phase protein that is up-regulated upon infection. *Proceedings of the National Academy of Sciences of the United States of America* 94, 12337-12342.
60. Yun, E.Y., Kang, S.W., Hwang, J.S., Goo, T.W., Kim, S.H., Jin, B.R., Kwon, O.Y., Kim, K.Y., 1999. Molecular cloning and characterization of a cDNA encoding a transferrin homolog from *Bombyx mori*. *Biological chemistry* 380, 1455-1459.
61. Alberts, B., Johnson, A., Lewis, J., 2002. *Electron-Transport Chains and Their Proton Pumps.*, 4th edition. ed. Garland Science, New York.
62. Arias, D.G., Marquez, V.E., Beccaria, A.J., Guerrero, S.A., Iglesias, A.A., 2010. Purification and characterization of a glutathione reductase from *Phaeodactylum tricorutum*. *Protist* 161, 91-101.

63. Arnold, K., Bordoli, L., Kopp, J., Schwede, T., 2006. The SWISS-MODEL workspace: a web-based environment for protein structure homology modelling. *Bioinformatics* 22, 195-201.
64. Arora, K., Ahmad, R., Srivastava, A.K., 2013. Purification and characterization of glutathione reductase (E.C. 1.8.1.7) from bovine filarial worms *Setaria cervi*. *Journal of parasitic diseases : official organ of the Indian Society for Parasitology* 37, 94-104.
65. Berkholz, D.S., Faber, H.R., Savvides, S.N., Karplus, P.A., 2008. Catalytic cycle of human glutathione reductase near 1 Å resolution. *Journal of molecular biology* 382, 371-384.
66. Birben, E., Sahiner, U.M., Sackesen, C., Erzurum, S., Kalayci, O., 2012. Oxidative stress and antioxidant defense. *The World Allergy Organization journal* 5, 9-19.
67. Boveris, A., 1977. Mitochondrial production of superoxide radical and hydrogen peroxide. *Advances in experimental medicine and biology* 78, 67-82.
68. Bradford, M.M., 1976. A rapid and sensitive method for the quantitation of microgram quantities of protein utilizing the principle of protein-dye binding. *Analytical biochemistry* 72, 248-254.
69. Cadenas, E., Davies, K.J., 2000. Mitochondrial free radical generation, oxidative stress, and aging. *Free radical biology & medicine* 29, 222-230.
70. Coban, T.A., Senturk, M., Ciftci, M., Kufrevioglu, O.I., 2007. Effects of some metal ions on human erythrocyte glutathione reductase: an in vitro study. *Protein and peptide letters* 14, 1027-1030.
71. Cook, P., 2014. The Worldwide Abalone Industry. *Modern Economy* 5, 1181-1186.
72. Day, R.M., Suzuki, Y.J., 2005. Cell proliferation, reactive oxygen and cellular glutathione. Dose-response : a publication of International Hormesis Society 3, 425-442.
73. Deponte, M., 2013. Glutathione catalysis and the reaction mechanisms of glutathione-dependent enzymes. *Biochimica et biophysica acta* 1830, 3217-3266.
74. Dolphin, D., Avramović, O., Poulson, R., 1989. *Glutathione reductase*. Wiley, the University of Michigan.
75. Elston, R., Lock wood, G.S., 1983. Pathogenesis of vibriosis in cultured juvenile red abalone, *Haliotis rufescens* Swainson. *Journal of Fish Diseases* 6, 111-128.
76. Erat, M., Demir, H., Sakiroglu, H., 2005. Purification of glutathione reductase from chicken liver and investigation of kinetic properties. *Applied biochemistry and biotechnology* 125, 127-138.
77. Erat, M., Sakiroglu, H., Ciftci, M., 2003. Purification and characterization of glutathione reductase from bovine erythrocytes. *Preparative biochemistry & biotechnology* 33, 283-300.
78. Evans, B., White, R.W., Elliott, N.G., 2000. Characterization of microsatellite loci in the Australian Blacklip abalone (*Haliotis rubra*, Leach). *Molecular ecology* 9, 1183-1184.
79. Flora, S.J., Mittal, M., Mehta, A., 2008. Heavy metal induced oxidative stress & its possible reversal by chelation therapy. *The Indian journal of medical research* 128, 501-523.
80. Gill, S.S., Anjum, N.A., Hasanuzzaman, M., Gill, R., Trivedi, D.K., Ahmad, I., Pereira, E., Tuteja, N., 2013. Glutathione and glutathione reductase: a boon in disguise for plant abiotic stress defense operations. *Plant physiology and biochemistry : PPB / Societe francaise de physiologie vegetale* 70, 204-212.
81. Goggin, C.L., Lester, R.J.G., 1995. Perkinsus, a protistan parasite of abalone in Australia: A review. *Marine and Freshwater Research* 46, 639 - 646

82. Hansen, T.N., Tonoki, H., McMicken, H., Smith, C.V., 1993. INHIBITION OF GLUTATHIONE-REDUCTASE ACTIVITY IN CHO CELLS BY ANTISENSE GENE TRANSFECTION INCREASES THEIR SENSITIVITY TO OXIDANT INJURY *Free radical biology & medicine* 15, 543-543.
83. Huang, C.Y., Liu, P.C., Lee, K.K., 2001. Withering syndrome of the small abalone, *Haliotis diversicolor supertexta*, is caused by *Vibrio parahaemolyticus* and associated with thermal induction. *Zeitschrift fur Naturforschung. C, Journal of biosciences* 56, 898-901.
84. Jones, D.P., 2002. Redox potential of GSH/GSSG couple: assay and biological significance. *Methods in enzymology* 348, 93-112.
85. Karplus, P.A., Schulz, G.E., 1987. Refined structure of glutathione reductase at 1.54 Å resolution. *Journal of molecular biology* 195, 701-729.
86. Klinbunga, S., Pripue, P., Khamnamtong, N., Puanglarp, N., Tassanakajon, A., Jarayabhand, P., Hirono, I., Aoki, T., Menasveta, P., 2003. Genetic diversity and molecular markers of the tropical abalone (*Haliotis asinina*) in Thailand. *Marine biotechnology* 5, 505-517.
87. Krohne-Ehrich, G., Schirmer, R.H., Untucht-Grau, R., 1977. Glutathione reductase from human erythrocytes. Isolation of the enzyme and sequence analysis of the redox-active peptide. *European journal of biochemistry / FEBS* 80, 65-71.
88. Kubo, A., Sano, T., Saji, H., Tanaka, K., Kondo, N., Tanaka, K., 1993. Primary Structure and Properties of Glutathione Reductase from *Arabidopsis thaliana*. *Plant and Cell Physiology* 34, 1259-1266.
89. Kunert, K.J., Cresswell, C.F., Schmidt, A., Mullineaux, P.M., Foyer, C.H., 1990. Variations in the activity of glutathione reductase and the cellular glutathione content in relation to sensitivity to methylviologen in *Escherichia coli*. *Archives of biochemistry and biophysics* 282, 233-238.
90. Lee, Y., De Zoysa, M., Whang, I., Lee, S., Kim, Y., Oh, C., Choi, C.Y., Yeo, S.Y., Lee, J., 2011. Molluscan death effector domain (DED)-containing caspase-8 gene from disk abalone (*Haliotis discus discus*): molecular characterization and expression analysis. *Fish & shellfish immunology* 30, 480-487.
91. Lee, Y.M., Lee, K.W., Park, H., Park, H.G., Raisuddin, S., Ahn, I.Y., Lee, J.S., 2007. Sequence, biochemical characteristics and expression of a novel Sigma-class of glutathione S-transferase from the intertidal copepod, *Tigriopus japonicus* with a possible role in antioxidant defense. *Chemosphere* 69, 893-902.
92. Liu, P.C., Chen, Y.C., Huang, C.Y., Lee, K.K., 2000. Virulence of *Vibrio parahaemolyticus* isolated from cultured small abalone, *Haliotis diversicolor supertexta*, with withering syndrome. *Letters in applied microbiology* 31, 433-437.
93. Livak, K.J., Schmittgen, T.D., 2001. Analysis of relative gene expression data using real-time quantitative PCR and the 2^{-ΔΔC(T)} Method. *Methods* 25, 402-408.
94. Loprasert, S., Whangsuk, W., Sallabhan, R., Mongkolsuk, S., 2005. The unique glutathione reductase from *Xanthomonas campestris*: gene expression and enzyme characterization. *Biochemical and biophysical research communications* 331, 1324-1330.
95. Marchler-Bauer, A., Lu, S., Anderson, J.B., Chitsaz, F., Derbyshire, M.K., DeWeese-Scott, C., Fong, J.H., Geer, L.Y., Geer, R.C., Gonzales, N.R., Gwadz, M., Hurwitz, D.I., Jackson, J.D., Ke, Z., Lanczycki, C.J., Lu, F., Marchler, G.H., Mullokandov, M., Omelchenko, M.V., Robertson, C.L., Song, J.S., Thanki, N., Yamashita, R.A., Zhang, D., Zhang, N., Zheng,

- C., Bryant, S.H., 2011. CDD: a Conserved Domain Database for the functional annotation of proteins. *Nucleic acids research* 39, D225-229.
96. Meister, A., 1988. Glutathione metabolism and its selective modification. *The Journal of biological chemistry* 263, 17205-17208.
97. Minami, Y., Kohama, T., Sekimoto, Y.J., Akasaka, K., Matsubara, H., 2003. Isolation and characterization of glutathione reductase from *Physarum polycephalum* and stage-specific expression of the enzyme in life-cycle stages with different oxidation-reduction levels. *The Journal of eukaryotic microbiology* 50, 317-323.
98. Mize, C.E., Langdon, R.G., 1962. Hepatic glutathione reductase. I. Purification and general kinetic properties. *The Journal of biological chemistry* 237, 1589-1595.
99. Muller, S., Gilberger, T.W., Fairlamb, A.H., Walter, R.D., 1997. Molecular characterization and expression of *Onchocerca volvulus* glutathione reductase. *The Biochemical journal* 325 (Pt 3), 645-651.
100. Munoz, C.M., van Meeteren, L.A., Post, J.A., Verkleij, A.J., Verrips, C.T., Boonstra, J., 2002. Hydrogen peroxide inhibits cell cycle progression by inhibition of the spreading of mitotic CHO cells. *Free radical biology & medicine* 33, 1061-1072.
101. Nakatsugawa, T., Nagai, T., Hiya, K., Nishizawa, T., Muroga, K., 1999. A virus isolated from juvenile Japanese black abalone *Nordotis discus discus* affected with amyotrophy. *Diseases of Aquatic Organisms* 36, 159-161.
102. Park, M., Shin, H.J., Lee, S.Y., Ahn, T.I., 2005. Characterization of a cDNA of peroxiredoxin II responding to hydrogen peroxide and phagocytosis in *Amoeba proteus*. *The Journal of eukaryotic microbiology* 52, 223-230.
103. Pettersson, P.L., Mannervik, B., 2001. The role of glutathione in the isomerization of delta 5-androstene-3,17-dione catalyzed by human glutathione transferase A1-1. *The Journal of biological chemistry* 276, 11698-11704.
104. Presnell, C.E., Bhatti, G., Numan, L.S., Lerche, M., Alkhateeb, S.K., Ghalib, M., Shammaa, M., Kavdia, M., 2013. Computational insights into the role of glutathione in oxidative stress. *Current neurovascular research* 10, 185-194.
105. Reed, D.J., 1985. Nitrosoureas. Academic Press, London.
106. Sanz, A., Stefanatos, R.K., 2008. The mitochondrial free radical theory of aging: a critical view. *Current aging science* 1, 10-21.
107. Seifried, H.E., Anderson, D.E., Fisher, E.I., Milner, J.A., 2007. A review of the interaction among dietary antioxidants and reactive oxygen species. *The Journal of nutritional biochemistry* 18, 567-579.
108. Seo, J.S., Lee, K.W., Rhee, J.S., Hwang, D.S., Lee, Y.M., Park, H.G., Ahn, I.Y., Lee, J.S., 2006. Environmental stressors (salinity, heavy metals, H₂O₂) modulate expression of glutathione reductase (GR) gene from the intertidal copepod *Tigriopus japonicus*. *Aquatic toxicology* 80, 281-289.
109. Sies, H., 1997. Oxidative stress: oxidants and antioxidants. *Experimental physiology* 82, 291-295.
110. Sipes, I.G., Wiersma, D.A., Armstrong, D.J., 1986. The role of glutathione in the toxicity of xenobiotic compounds: metabolic activation of 1,2-dibromoethane by glutathione. *Advances in experimental medicine and biology* 197, 457-467.
111. Tamura, K., Stecher, G., Peterson, D., Filipski, A., Kumar, S., 2013. MEGA6: Molecular Evolutionary Genetics Analysis version 6.0. *Molecular biology and evolution* 30, 2725-2729.

112. Tekman, B., Ozdemir, H., Senturk, M., Ciftci, M., 2008. Purification and characterization of glutathione reductase from rainbow trout (*Oncorhynchus mykiss*) liver and inhibition effects of metal ions on enzyme activity. *Comparative biochemistry and physiology. Toxicology & pharmacology* : CBP 148, 117-121.
113. Thompson, J.D., Higgins, D.G., Gibson, T.J., 1994. CLUSTAL W: improving the sensitivity of progressive multiple sequence alignment through sequence weighting, position-specific gap penalties and weight matrix choice. *Nucleic acids research* 22, 4673-4680.
114. Toppo, S., Flohe, L., Ursini, F., Vanin, S., Maiorino, M., 2009. Catalytic mechanisms and specificities of glutathione peroxidases: variations of a basic scheme. *Biochimica et biophysica acta* 1790, 1486-1500.
115. Valko, M., Rhodes, C.J., Moncol, J., Izakovic, M., Mazur, M., 2006. Free radicals, metals and antioxidants in oxidative stress-induced cancer. *Chemico-biological interactions* 160, 1-40.
116. Vitale, A.M., Monserrat, J.M., Castilho, P., Rodriguez, E.M., 1999. Inhibitory effects of cadmium on carbonic anhydrase activity and ionic regulation of the estuarine crab *Chasmagnathus granulata* (Decapoda, Grapsidae). *Comparative biochemistry and physiology. Part C, Pharmacology, toxicology & endocrinology* 122, 121-129.
117. Volodymyr, I.L., 2012 *Glutathione Homeostasis and Functions: Potential Targets for Medical Interventions*. *Journal of Amino Acids* 2012, 26.
118. Wan, Q., Whang, I., Lee, J., 2012. Molecular and functional characterization of HdHSP20: a biomarker of environmental stresses in disk abalone *Haliotis discus discus*. *Fish & shellfish immunology* 33, 48-59.
119. Warren, L.D., PyMOL: An Open-Source Molecular Graphics Tool.
120. Yan, J., Meng, X., Wancket, L.M., Lintner, K., Nelin, L.D., Chen, B., Francis, K.P., Smith, C.V., Rogers, L.K., Liu, Y., 2012. Glutathione reductase facilitates host defense by sustaining phagocytic oxidative burst and promoting the development of neutrophil extracellular traps. *Journal of immunology* 188, 2316-2327.
121. Yan, J., Ralston, M.M., Meng, X., Bongiovanni, K.D., Jones, A.L., Benndorf, R., Nelin, L.D., Joshua Frazier, W., Rogers, L.K., Smith, C.V., Liu, Y., 2013. Glutathione reductase is essential for host defense against bacterial infection. *Free radical biology & medicine* 61, 320-332.